



Global sensitivities of reactive N and S gas and particle concentrations and deposition to precursor emissions reductions

Yao Ge^{1,2}, Massimo Vieno², David S. Stevenson³, Peter Wind⁴, Mathew R. Heal¹

¹ School of Chemistry, University of Edinburgh, Joseph Black Building, David Brewster Road, Edinburgh, EH9 3FJ, UK

5 ² UK Centre for Ecology & Hydrology, Bush Estate, Penicuik, Midlothian, EH26 0QB, UK

³ School of GeoSciences, University of Edinburgh, Crew Building, Alexander Crum Brown Road, Edinburgh, EH9 3FF, UK

⁴ The Norwegian Meteorological Institute, Henrik Mohns Plass 1, 0313, Oslo, Norway

Correspondence to: Yao Ge (Y.Ge-7@sms.ed.ac.uk), Mathew R. Heal (M.Heal@ed.ac.uk)

Abstract. The reduction of fine particles (PM_{2.5}) and reactive N (N_r) and S (S_r) species is a key objective for air pollution control policies because of their major adverse effects on human health, ecosystem diversity, and climate. The sensitivity of global and regional N_r, S_r, and PM_{2.5} to 20% and 40% individual and collective reductions in anthropogenic emissions of NH₃, NO_x, and SO_x (with respect to a 2015 baseline) is investigated using the EMEP MSC-W atmospheric chemistry transport model with WRF meteorology. Regional comparisons reveal that the individual emissions reduction has multiple co-benefits and small disbenefits on different species, and those effects are highly geographically variable. Reductions in NH₃ emissions are effective at decreasing NH₃ concentrations and deposition but much less so for NH₄⁺. A 40% NH₃ emissions reduction decreases regional average NH₃ concentrations by 47-49%, while sensitivities of NH₄⁺ concentrations decrease in the order Euro_Medi (Europe and Mediterranean, 18%), East Asia (15%), North America (12%), and South Asia (4%), reflecting the increasing regional ammonia-richness. A disbenefit is the increased SO₂ concentrations in these regions (10-16% for 40% NH₃ emissions reductions) because reduced NH₃ levels decrease SO₂ deposition by altering atmospheric acidity. The 40% NO_x emissions reductions decrease NO_x concentrations in East Asia by 45%, Euro_Medi and North America by ~38%, and South Asia by 22%, whilst decreases in fine NO₃⁻ are regionally reversed, which is related to enhanced O₃ levels in East Asia (and also, but by less, in Euro_Medi), and decreased O₃ levels in South Asia (and also, but by less, in North America). Consequently, the oxidation of NO_x to NO₃⁻ and of SO₂ to SO₄²⁻ is enhanced in East Asia but decreased in South Asia, which in East Asia causes a more effective decrease in NO_x and SO₂ but a less effective decrease in NO₃⁻ and even an increase in SO₄²⁻; in South Asia it causes a less effective decrease in NO_x and an increase in SO₂ but a more effective decrease in NO₃⁻ and SO₄²⁻. For regional policy making, it is thus important to reduce NH₃, NO_x and SO_x emissions together and/or go for stronger reductions to minimise such adverse effects in East Asia and Euro_Medi. Reductions in SO_x emissions are slightly more effective for SO₂ than SO₄²⁻. A disbenefit is that SO_x emissions reductions increase NH₃ total deposition and ecosystem eutrophication (~12% increase for 40% emissions reduction). PM_{2.5} mitigation in South Asia is most sensitive to 40% SO_x reduction (3.10 µg m⁻³, 10%) and least sensitive to NH₃ reduction (0.29 µg m⁻³, 1%), which is because South Asia is so ammonia-rich that reducing NH₃ has little impact. The most effective measure for North America is reducing NO_x emissions with an 8% (0.63 µg m⁻³) decrease in PM_{2.5} in response to a 40% reduction. In Euro_Medi, the sensitivities of PM_{2.5} to 40% individual emissions reductions range 5-8% (0.55-0.82 µg m⁻³). In the UK and Scandinavia PM_{2.5} is more sensitive to NH₃, in central Europe it is more sensitive to NO_x, while in the Mediterranean it is more sensitive to SO_x. In East Asia, reductions in SO_x, NO_x and NH₃ emissions are almost equally effective with PM_{2.5} sensitivities to 40% reductions of 7-8% (1.89-2.33 µg m⁻³). Due to the varying contributions of SIA, PM_{2.5} sensitivities to 40% collective reductions in all 3 precursors decrease in the order East Asia (20%), Euro_Medi and North America (17%), South Asia (13%). The geographically-varying non-linear chemical responses of N_r, S_r, and PM_{2.5} to emissions reductions revealed by this work show the importance of both prioritising emissions strategies in different regions and combining several precursor reductions together to maximise the policy effectiveness.



40 1 Introduction

Reactive N (N_r) and S (S_r) species are critical determinants of air quality. A substantial proportion of ambient $PM_{2.5}$ (particulate matter with aerodynamic diameter $\leq 2.5 \mu m$) is secondary inorganic aerosol (SIA) formed from chemical reactions of emissions of the precursor gases NH_3 , NO_x (NO and NO_2) and SO_x (sulfur oxides, mainly SO_2) (Behera et al., 2013; Weber et al., 2016; Vasilakos et al., 2018; Nenes et al., 2020). $PM_{2.5}$ is consistently associated with elevated risk of all-cause mortality and other adverse health impacts (Hart et al., 2015; Chen et al., 2017; Chen et al., 2018a; Karimi et al., 2019; Stieb et al., 2020). The gases NO_2 and SO_2 are also direct health pollutants. In addition, oxidized N (e.g., NO_x , HNO_3 , and NO_3^- , collectively abbreviated as OXN) and reduced N (e.g., NH_3 and NH_4^+ , collectively abbreviated as RDN) species are powerful nutrients for plants and microorganisms, whose deposition leads to eutrophication and loss of ecosystem biodiversity (Erisman et al., 2005; Bergström and Jansson, 2006; Sun et al., 2017; Kharol et al., 2018). The severity of the adverse effects of N deposition is determined not only by the total quantity but also its form. Many studies show different N deposition components have varying toxicity to different plants, dry deposition of NH_3 is particularly deleterious for example (Van Herk et al., 2003; Sheppard et al., 2011; Sutton et al., 2014, 2020; Pescott et al., 2015) Deposition of oxidized S (i.e., SO_2 and SO_4^{2-} , collectively abbreviated as OXS) also greatly influences precipitation acidity (Lu et al., 2010; Aas et al., 2019; McHale et al., 2021). These observations put greater emphasis on mitigation of certain deposition components.

The East Asia, South Asia, Euro_Medi (Europe and Mediterranean) and North America regions have high population density and high N_r and S_r pollution. Historically, Europe and North America were the dominant emissions regions, suffering severe air pollution until the late 20th century. However, the combination of emissions controls for SO_x and NO_x in these two regions and rapid industrialisation elsewhere means that emissions in East and South Asia now dominate globally (Weber et al., 2016; NEC, 2019; Fowler et al., 2020), although China, in particular, is now implementing effective SO_x and NO_x emissions controls (Liu et al., 2016; Hoesly et al., 2018; Zheng et al., 2018; Meng et al., 2022). In contrast, a lack of action on NH_3 emissions in most countries, coupled with the growth in agriculture to feed a rising global population, means that global NH_3 emissions continue to grow (Heald et al., 2012; Fowler et al., 2015; Aksoyoglu et al., 2020). As a result, ambient N_r and S_r pollution remains a major health and environmental concern in most regions. The European Environmental Agency reported that 97% of the urban population in the European Union in 2019 was exposed to annual mean concentrations of $PM_{2.5}$ above the latest World Health Organization (WHO) air quality guideline of $5 \mu g m^{-3}$ (EEA, 2021; WHO, 2021), whilst the United States Environmental Protection Agency reported that for the period 2014–2016 only 10% of its 429 monitoring sites had $PM_{2.5}$ concentrations $< 6.0 \mu g m^{-3}$ (USEPA, 2017). Combining satellite retrievals, chemistry model simulations, and ground level measurements, Ma et al. (2014) and Brauer et al. (2016) showed that in 2013 the majority of the East and South Asia population lived in areas where annual mean $PM_{2.5}$ concentrations exceeded the WHO Interim Target 1 of $35 \mu g m^{-3}$ (WHO, 2021). Furthermore, as mitigation of NO_x emissions in recent years has been more effective than for NH_3 , deposition of RDN is now increasingly responsible for the exceedances of N critical loads for eutrophication in many regions (Jovan et al., 2012; Chen et al., 2018b; Simpson et al., 2020; Yi et al., 2021; Jonson et al., 2022).

Understanding the sensitivities of $PM_{2.5}$, N_r and S_r pollution to emissions reductions is complicated not only by the substantial regional heterogeneity in relative emissions but also by the substantial meteorological heterogeneity influencing the chemistry and deposition. This necessitates use of atmospheric chemistry transport models (ACTMs) designed to simulate the underlying physical–chemical processes linking emissions, dispersion, chemical reactions, and deposition of atmospheric components. Previous ACTM studies have provided insight into the complexities of sensitivities of $PM_{2.5}$ and its SIA components to changes in emissions in different regions that measurements cannot reveal. For example, using the GEOS-Chem model, Wang et al. (2013) showed that SIA concentrations in 2015 decreased in South China and Sichuan Basin but increased in North China compared to their 2006 levels in response to -16% SO_2 and $+16\%$ NO_x emissions changes (no change in NH_3 emissions) from 2006 to 2015 according to China's 12th Five-Year Plan, but if NH_3 emissions increase by $+16\%$ (based on their growth rate from 2006 to 2015), the SIA reduction due to SO_2 reduction will be totally offset in all regions because of



the elevated NH_3NO_3 formation, demonstrating the importance of NH_3 control on China's SIA mitigation. Pommier et al. (2018) reported substantial projected growth in emissions in India between 2011 and 2050, amounting to 304% for SO_x , 287% for NMVOC, 162% for NO_x , 100% for primary $\text{PM}_{2.5}$, and 60% for CO and NH_3 , leading to increases in annual mean $\text{PM}_{2.5}$ and O_3 concentrations of 67% and 13% respectively. In the UK, results from EMEP4UK model simulations for 2010 emissions and meteorology indicated that NH_3 emissions reductions are the most effective single-component control (compared to individual reductions in NO_x , SO_x , and primary $\text{PM}_{2.5}$) on area-weighted $\text{PM}_{2.5}$, whilst weighting by population placed greater emphasis on reductions in emissions of primary $\text{PM}_{2.5}$ (Vieno et al., 2016). Holt et al. (2015) used GEOS-Chem to investigate $\text{PM}_{2.5}$ sensitivities in the United States to NO_x , SO_2 , and NH_3 emissions reductions between two sets of scenarios representing a 2005 baseline (high emissions) and a 2012 analogue (low emissions) for both summer and winter, with the national total emissions exhibiting a 62% decrease in SO_2 , a 42% decrease in NO_x , and a 1% increase in NH_3 from 2005 to 2012. They found larger sensitivities of $\text{PM}_{2.5}$ to NO_x reductions in winter than in summer in parts of the northern Midwest because $\text{PM}_{2.5}$ is more nitrate-limited in the low emissions case, and that lower NO_x and SO_2 emissions in 2012 led to larger $\text{PM}_{2.5}$ sensitivity to SO_2 compared to 2005 since lower NO_x emissions enhance the relative importance of aqueous-phase SO_2 oxidation.

These studies analysed N_r and S_r responses to precursor emissions reductions in the early 2000s and in specific regions, but do not provide a global view of sensitivities to the same reductions everywhere. Given the considerable emissions changes in global and regional NH_3 , NO_x , and SO_x in recent years (Hoesly et al., 2018; Kurokawa and Ohara, 2020), our understanding of the current chemical climate for N_r and S_r reactions on global and regional scale and how it affects responses of $\text{PM}_{2.5}$, N_r and S_r species to various emissions reductions should be updated. This is the motivation for the work presented here, which provides a global picture of the effectiveness of NH_3 , NO_x , and SO_x emissions reductions for mitigating both concentrations and deposition of N_r and S_r pollutants. We used the EMEP MSC-W ACTM to simulate the global domain based on global emissions and meteorology in 2015, which enables a regional comparison to be conducted with inherently consistent simulations. The focus here is on annual means, as these are the long-term metric within global and regional air quality standards. We first describe the model set-up and performance and the sensitivity experiments used to simulate responses of $\text{PM}_{2.5}$, N_r and S_r species to 20% and 40% reductions in gaseous precursor emissions (Sect. 2). Section 3 details the global and regional concentration and deposition changes in components of RDN, OXN, OXS, and $\text{PM}_{2.5}$ between baseline and emissions reduction scenarios. Section 4 discusses key processes that determine the benefits and disbenefits of emissions reductions and how they vary geographically, and the implications of our findings for policy making.

2 Methods

2.1 Model set-up and performance

The EMEP MSC-W (European Monitoring and Evaluation Programme Meteorological Synthesizing Centre – West) open-source atmospheric chemistry transport model (<https://www.emep.int>, last access: 8 August 2022) is a three-dimensional Eulerian model widely used for both scientific research and policy development (Bergström et al., 2014; Jonson et al., 2017; Pommier et al., 2018; McFiggans et al., 2019; Karl et al., 2019; Pommier et al., 2020; Jonson et al., 2022). Version rv4.34 was used here. A detailed technical description of EMEP MSC-W rv4.0 is documented in Simpson et al. (2012). A series of overviews of model updates from version rv4.0 to rv4.34 is documented in annual EMEP status reports (Simpson et al., 2013; Tsyro et al., 2014; Simpson et al., 2015, 2016, 2017, 2018, 2019, 2020b). Meteorology for 2015 was derived from the Weather Research and Forecasting model (WRF; <https://www.wrf-model.org>; <https://github.com/wrf-model/WRF/releases/tag/v4.2.2>, last access: 8 August 2022) version 4.2.2. The coupled EMEP-WRF system has been tested and applied to many regional and global studies (Vieno et al., 2010, 2014, 2016; Werner et al., 2018; Chang et al., 2020; Gu et al., 2021).

Detailed global EMEP-WRF configurations used in this work are presented in Ge et al. (2021b, 2022). In brief, the global domain has a horizontal resolution of $1^\circ \times 1^\circ$ and 21 terrain-following vertical layers from the surface up to 100 hPa. The



height of the lowest model layer is around 45 m. The model outputs of surface concentrations are adjusted to correspond to 3
125 m above ground level in order to provide concentrations at heights more typical of ambient measurements and human exposure
(Simpson et al., 2012). The aerosol module is the Equilibrium Simplified Aerosol Model V4 (EQSAM4clim), which
parameterizes a full gas–liquid–solid partitioning scheme for semi-volatile and non-volatile mixtures. Details are described in
Metzger et al. (2016, 2018). Dry deposition of gaseous species and aerosol components to the ground surface is simulated
utilizing deposition velocity as described in Simpson et al. (2012, 2020). The parameterisation of wet deposition incorporates
130 both in-cloud and below-cloud scavenging of gases and particles (Berge and Jakobsen, 1998; Simpson et al., 2012).

The global model evaluation of N_r and S_r concentrations and wet deposition from this model configuration for 2010 and
2015 against measurements from 10 ambient monitoring networks is documented in Ge et al. (2021b) and demonstrates the
model's capability for capturing the spatial and seasonal variations of NH_3 , NH_4^+ , NO_2 , HNO_3 , NO_3^- , SO_2 , and SO_4^{2-} in East
Asia, Southeast Asia, Europe, and North America. As an example, the correlation coefficients between model and
135 measurement annual mean concentrations for most species in 2015 are ≥ 0.78 , and for annual wet deposition of RDN and
OXN are 0.78 and 0.63 respectively. This is in spite of inherent uncertainty in both model and measurements and differences
in their spatial representativeness.

2.2 Emissions and model experiments

Baseline emissions for 2015 were from the ECLIPSE V6 (Evaluating the CLimate and Air Quality ImPacts of Short-livEd
140 Pollutant) inventory, available at <https://previous.iiasa.ac.at/web/home/research/researchPrograms/air/ECLIPSEv6b.html> (last
access: 8 August 2022). Monthly emissions profiles derived from EDGAR (Emission Database for Global Atmospheric
Research, v4.3.2 datasets, available at https://edgar.jrc.ec.europa.eu/dataset_temp_profile) time series (Crippa et al., 2020)
were applied to the ECLIPSE annual emissions of SO_2 , NO_2 , NH_3 , CO , CH_4 , NMVOC, primary $PM_{2.5}$ and coarse particles.
Detailed implementation procedures including the re-assignment of ECLIPSE emissions sectors to EMEP sectors and the
145 calculation of temporal profiles at a given country for a given pollutant are described in Ge et al. (2021b).

A baseline simulation and a set of 8 sensitivity experiments were conducted for emissions and meteorology for 2015.
The model experiments applied 20% and 40% reductions to global anthropogenic emissions of NH_3 , NO_x , SO_x from all
sectors both individually and collectively (i.e., reductions applied to all 3 species simultaneously). All other emissions,
including natural emissions such as dimethyl sulfide from oceans, lightning NO_x , and soil NO_x , were left unchanged.

150 2.3 Definition of world regions

We compared the sensitivities to the emissions reductions of $PM_{2.5}$, N_r and S_r species concentrations and depositions in
the four world regions of East Asia, South Asia, Euro_Medi, and North America defined in Fig. 1 (and listed in Table S1).
These are based on regions used by the Intergovernmental Panel on Climate Change and as rationalised in Iturbide et al. (2020).
All four regions are densely populated and have high N_r and S_r pollution as reported by Ge et al. (2022).

155

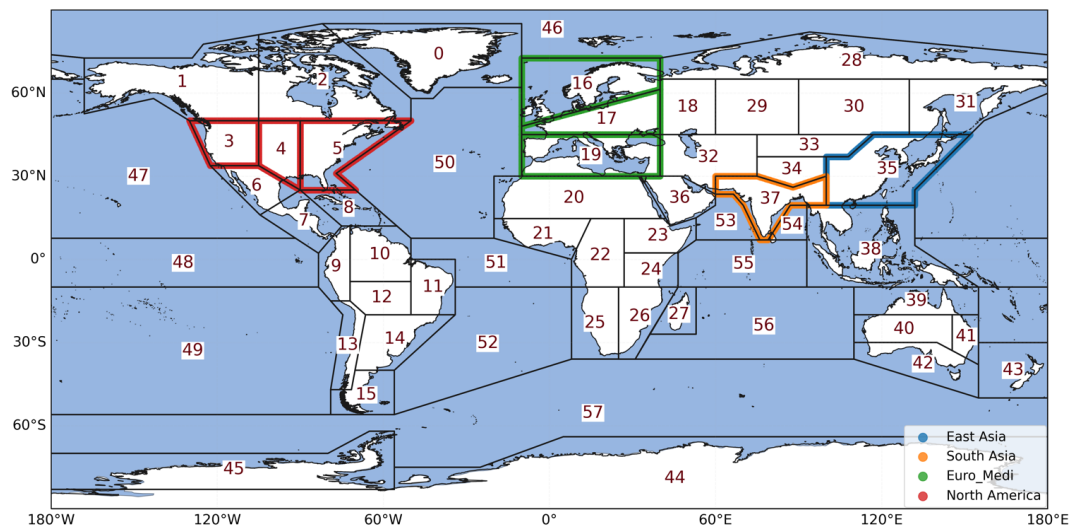


Figure 1: The boundaries of the 4 world regions used in this study, which are based on the IPCC reference regions described in Iturbide et al. (2020).

3 Results

160 3.1 Sensitivities of N_r and S_r gas and aerosol concentrations

The simulated global baseline 2015 annual mean surface concentrations of N_r and S_r have been discussed in detail in Ge et al. (2022). Here we analyse the sensitivities of the modelled surface concentrations to SIA precursor emissions reductions for RDN, OXN and OXS components. Sensitivities differ according to consideration of primary or secondary components and show great geographical variation.

165 3.1.1 RDN

Figure 2 shows the spatial variations in the sensitivities of NH_3 and NH_4^+ annual mean surface concentrations to 20% and 40% emissions reductions in NH_3 , NO_x , and SO_x individually, and collectively. Regional average sensitivities in East Asia, South Asia, Euro_Medi, and North America are summarised in Fig. 3 and Table S2. Steeper gradients in Fig. 3 correspond to greater concentration changes (sensitivities).

170 From these figures, it is clear that whilst reducing emissions of NH_3 (and all 3 precursors together) decrease NH_3 concentrations efficiently, reducing emissions of NO_x and SO_x lead to increases in NH_3 concentrations, particularly over densely populated areas. The maximum reduction in model grid NH_3 concentration across all scenarios reaches $16.6 \mu g m^{-3}$ (44% change relative to baseline; expressed similarly hereafter) and occurs over East Asia in response to a 40% reduction in NH_3 emissions. The largest increase in NH_3 concentration ($1.51 \mu g m^{-3}$, 22%) arises in Southeast Asia under the 40% SO_x emissions reduction scenario. Lower NO_x and SO_x emissions decrease the concentration of acidic species available to react with NH_3 to form NH_4^+ aerosol, so more of the emitted NH_3 stays in the gas phase. Other studies have likewise shown that reductions in SO_2 or NO_x emissions are an important contributor to the growth in tropospheric NH_3 concentrations globally and regionally (Saylor et al., 2015; Warner et al., 2017; Liu et al., 2018; Yu et al., 2018).

180 In East Asia and North America, NH_3 concentrations increase similarly for either NO_x or SO_x reductions (Fig. 3), but in South Asia and Euro_Medi, NH_3 concentrations increase more with SO_x reductions than with NO_x reductions, which reflects the larger contribution of $(NH_4)_2SO_4$ than NH_4NO_3 to SIA in the latter two regions. However, the increase in NH_3 concentrations is relatively small compared to the extent of NO_x and SO_x emissions reductions: 40% reductions in emissions

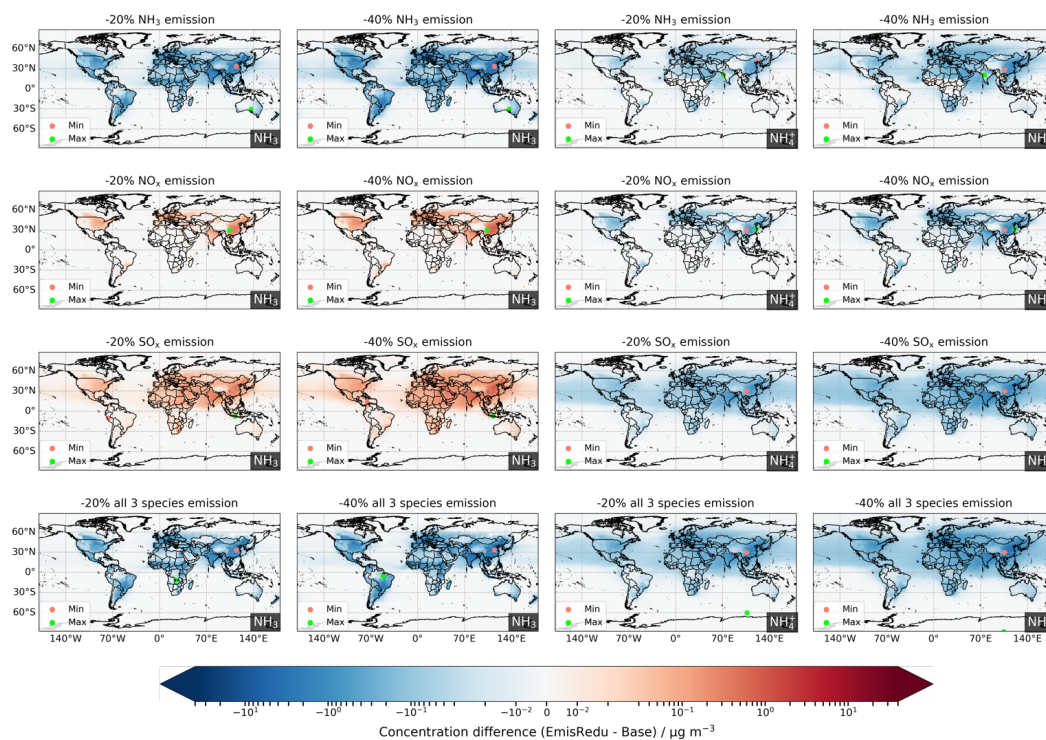


of NO_x or SO_x only increases NH_3 concentrations in the 4 regions by 2-6% or 6-9%, respectively (Fig. 3, Table S2). The globally averaged increases in NH_3 concentrations for 40% reductions in NO_x or SO_x emissions are 3% and 9%, respectively. Nevertheless, NH_3 concentration decrease resulting from reductions in NH_3 emissions is offset by simultaneous effects of NO_x and SO_x emissions reductions when all 3 precursors are reduced together, as the sensitivities of regional average NH_3 concentrations to 40% reductions in all 3 precursor emissions (38-39% across the four regions) are smaller than their sensitivities to 40% reductions in NH_3 emissions on its own (47-49%). It is also noteworthy that the sensitivities of regional average NH_3 concentrations are essentially linear through 20% and 40% emissions reductions, irrespective of precursor, although the sensitivities are different between regions.

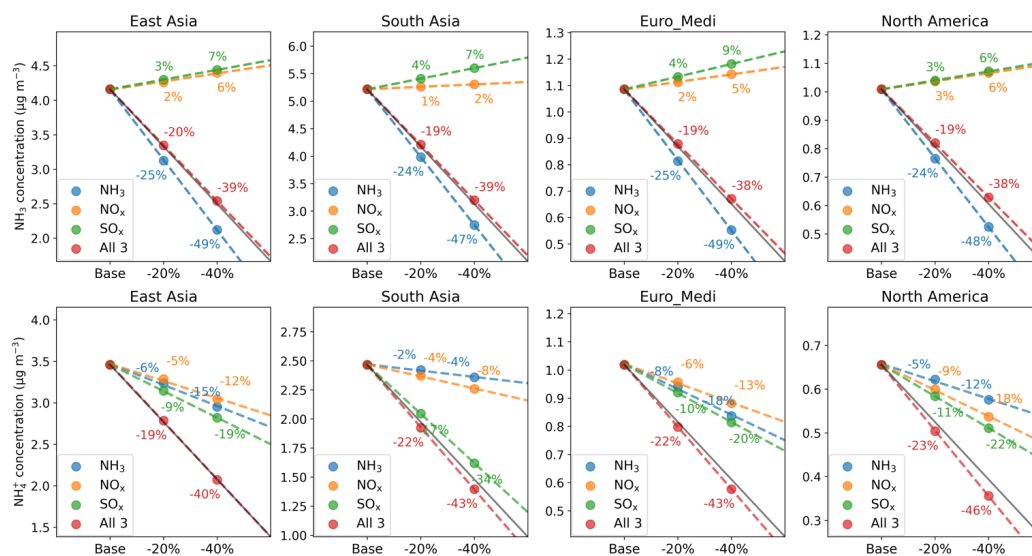
In contrast to NH_3 , concentrations of NH_4^+ always decrease when an SIA precursor emission is reduced. Figure 2 shows that NH_4^+ concentrations in the most densely populated continents (e.g., eastern China, India, Europe, eastern America) respond strongly to emissions reductions in each SIA precursor, whilst they only respond to SO_x emissions reductions over oceans. This is related to the production of marine sulfate aerosol from dimethyl sulfide (DMS) and the lack of significant oceanic NO_x emissions sources, which means only $(\text{NH}_4)_2\text{SO}_4$ formation is important in marine SIA chemistry.

In addition, the impacts of NH_3 and SO_x emissions reductions on NH_4^+ concentrations over North Africa are significantly greater than from NO_x emissions reductions, indicating a dominance of $(\text{NH}_4)_2\text{SO}_4$ within SIA in this region. This is consistent with the results reported by Ge et al. (2022). They showed that large areas in North Africa are characterised by the SO_4^{2-} -rich chemical domain for SIA formation, which means that NH_3 is predominantly taken up by SO_4^{2-} , leaving no free NH_3 to react with HNO_3 to form NH_4NO_3 . Given that emissions reductions in all three precursors individually lead to reductions in NH_4^+ concentrations, it is not surprising that the greatest simulated NH_4^+ reduction ($5.87 \mu\text{g m}^{-3}$ (43%) in East Asia) arises for the scenario with 40% reductions in all 3 precursors collectively.

Figure 3 also shows that NH_4^+ sensitivities are essentially linear for emissions reductions to 40%, although responses again vary slightly with region. Among individual precursor reduction scenarios, regional average NH_4^+ concentrations in East Asia and Euro_Medi are most sensitive to SO_x emissions reductions and least sensitive to NO_x reductions, while NH_4^+ concentrations in North America are most sensitive to SO_x reductions and least sensitive to NH_3 reductions. In South Asia, NH_4^+ is characterised by strong sensitivity to SO_x emissions reductions but only relatively small sensitivities to NO_x and NH_3 emissions reductions. In the scenario of all 3 species reductions, all regions show relative sensitivities close to the one-to-one line. Another important observation from Fig. 3 is that reductions in NH_4^+ (4-18%) in response to a 40% NH_3 emissions reduction are much smaller than reductions of NH_3 concentrations (47-49%) in these regions, which reflects the fact that these regions are so ammonia-rich that reducing NH_3 emissions only has limited effects on NH_4^+ concentrations.



215 **Figure 2: Changes in NH_3 and NH_4^+ annual surface concentrations for 20% and 40% emissions reductions in NH_3 , NO_x , and SO_x individually and collectively. Red and green dots in each map locate the minimum and maximum difference, respectively.**



220 **Figure 3: The absolute and relative sensitivities of regionally-averaged annual mean surface concentrations of NH_3 (upper row) and NH_4^+ (lower row) to 20% and 40% emissions reductions in NH_3 (blue), NO_x (orange) and SO_x (green) individually, and collectively (red), for the four regions defined in Fig. 1. The solid grey line in each panel illustrates the one-to-one relative response to emissions reductions, whilst the coloured dashed lines are the linear regressions through each set of three model simulations and illustrate the actual responses to emissions reductions of a given precursor. The numbers show the corresponding relative responses to each emissions reduction (with respect to baseline).**



3.1.2 OXN

225 Figure 4 shows the spatial variations in the sensitivities of NO_x and fine nitrate annual mean surface concentrations to 20% and 40% emissions reductions in NH_3 , NO_x , and SO_x individually, and collectively. Regional average sensitivities in East Asia, South Asia, Euro_Medi, and North America are summarised in Fig. 5 and Table S3. Equivalent global maps and regional sensitivity plots for the responses of HNO_3 and coarse nitrate to the same emissions reductions are presented in Figs. S1 and S2 and Table S3.

230 In contrast to surface NH_3 , whose concentrations are sensitive to reductions in emissions of each of NH_3 , NO_x and SO_x , surface NO_x concentrations only respond to NO_x emissions reductions and have negligible sensitivity to NH_3 and SO_x emissions reductions. The 20% and 40% reductions in NO_x emissions yield a global maximum of $25.6 \mu\text{g m}^{-3}$ (22%) and $51.3 \mu\text{g m}^{-3}$ (44%) reductions in surface NO_x concentrations over East Asia. The globally averaged reductions in NO_x concentrations for 20% and 40% reductions in NO_x emissions are 15% and 30% respectively (same values for simultaneous reductions in all
235 3 precursors), whereas the sensitivities for NH_3 and SO_x emissions reduction are all 0% (Table S3).

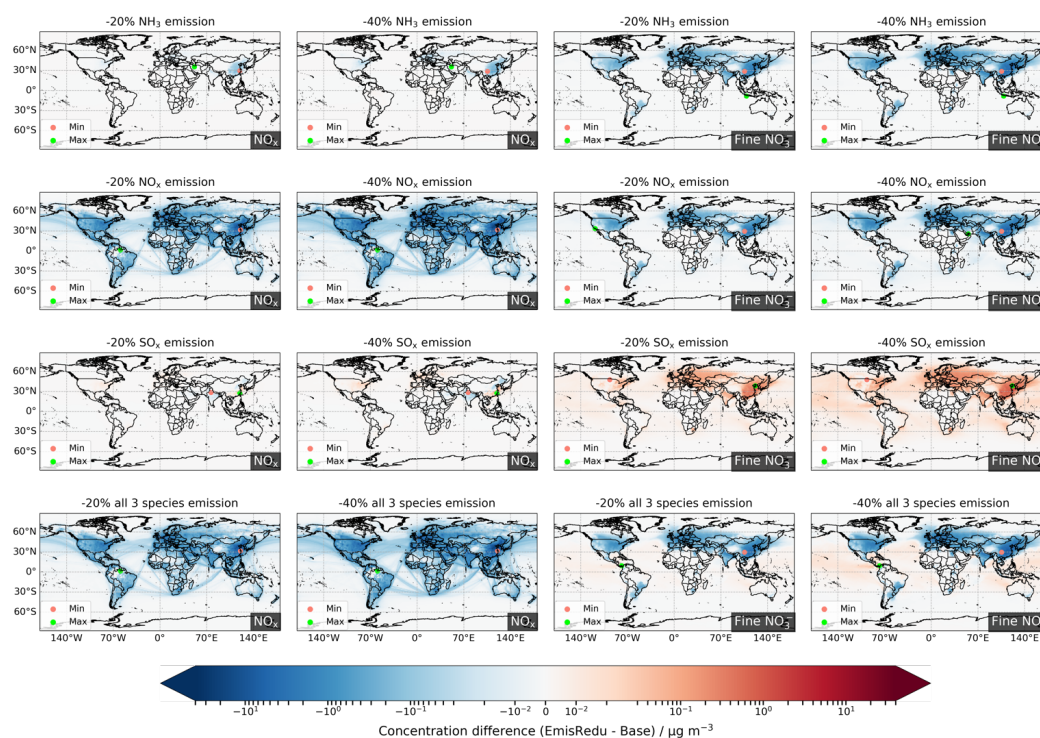
Regionally (Fig. 5), East Asia shows the largest decreases in NO_x concentrations (45%) in response to 40% NO_x emissions reductions, followed by Euro_Medi and North America (36-38%), and South Asia (23%). These regional differences in sensitivities to NO_x emissions are due to regional differences in oxidation chemistry climate. Figure S3 shows the changes in annual mean surface concentrations of O_3 for the 8 emissions reduction scenarios. Concentrations of O_3 in eastern China, western and central Europe, and north-eastern US increase as NO_x emissions reduce, while O_3 in the rest of the world decreases as NO_x emissions reduce. In East Asia, the increased oxidant levels enhance NO_x chemical removal and results in a greater than one-to-one relative decrease in NO_x concentrations with NO_x emissions reductions. Consequently, the decrease in fine nitrate in East Asia is offset by enhanced chemical production, which leads to a lower than one-to-one sensitivity (e.g., a 40% reduction in NO_x emissions gives a 33% decrease in fine NO_3^-). In contrast, decreased oxidant levels in South Asia decrease
240 the oxidation of NO_x , which partially offsets the decrease in NO_x concentrations induced by emissions reductions, causing a more efficient reduction in fine NO_3^- concentrations than in NO_x in this region. The variation in regional atmospheric oxidising capacity also alters the SO_4^{2-} formation processes; discussions of this are presented in Sect.3.1.3 and Sect. 4. The situation is more complex for Euro_Medi and North America as these regions include both positive and negative changes in O_3 concentrations with NO_x emissions reductions (Fig. S3) and they are not as NO_x -rich as East Asia and South Asia. The effects of changes in oxidant levels on NO_x and fine NO_3^- concentrations are therefore more localised and less apparent in regional averages. Clappier et al. (2021) reported this effect to be most distinct in the Po basin (Italy), western Germany, and Netherlands in Europe, whilst for the United States, Tsimpidi et al. (2008) showed it only becomes pronounced in the north east, both of which are consistent with our results.

For secondary OXN species, the sensitivities of HNO_3 and fine and coarse NO_3^- to individual reductions in emissions of
255 NH_3 , NO_x and SO_x are closely associated with SIA formation chemistry. The principal observation from Fig. 4 is that concentrations of fine NO_3^- in all four regions decrease with reduced NH_3 and NO_x emissions but increase with reduced SO_x emissions. This is because H_2SO_4 and HNO_3 compete in their reactions with NH_3 , and $(\text{NH}_4)_2\text{SO}_4$ is formed preferably over NH_4NO_3 . Reductions in NH_3 emissions cause the equilibrium between HNO_3 and NH_3 to shift away from NH_4NO_3 and therefore to a decrease in fine NO_3^- concentrations but to an increase in HNO_3 and coarse NO_3^- concentrations (Fig. S1).
260 Reductions in NO_x emissions decrease HNO_3 and fine and coarse NO_3^- concentrations globally. Although the increased oxidant levels that arise in some regions following NO_x emissions reductions enhance the chemical formation of these secondary species (as discussed above), NO_x emissions reductions of 20% and 40% are substantial enough to mean that the lower availability of NO_x to form NO_3^- dominates the impact on NO_3^- concentrations compared with the enhancement in oxidising capacity. Reduced SO_x emissions leave more NH_3 to equilibrate with HNO_3 to form NH_4NO_3 , leading to an increase in fine
265 NO_3^- concentrations but to a decrease in coarse NO_3^- concentrations as the former takes more HNO_3 . It is notable that the increase in fine NO_3^- concentrations is relatively small compared to the extent of SO_x emissions reductions. For example, the



maximum increase in fine NO_3^- resulting from 40% reductions in SO_x emissions is $1.71 \mu\text{g m}^{-3}$ (16%), in East Asia. The regional average increases in fine NO_3^- concentrations for 40% SO_x emissions reductions are 8% in East Asia, South Asia, and Euro_Medi, and 4% in North America.

270 The differences in regional average sensitivities of HNO_3 and fine and coarse NO_3^- are highlighted more clearly in Fig. 5 and Fig. S2. Fine NO_3^- in East Asia is equally sensitive to NO_x and NH_3 emissions reductions (33% and 32% decreases for 40% NO_x and NH_3 emissions reductions respectively), while it is more sensitive to NO_x emissions reductions than to NH_3 emissions reductions in South Asia (45% and 39%), Euro_Medi (41% and 33%), and North America (42% and 26%). In terms of absolute concentration changes, the reductions in fine NO_3^- over East Asia in response to 40% NH_3 and NO_x emissions reductions (1.62 -1.65 $\mu\text{g m}^{-3}$) are more than 3 times larger than reductions in other regions (0.23 - 0.47 $\mu\text{g m}^{-3}$). On the other hand, if NH_3 emissions are reduced then the increases in HNO_3 and coarse NO_3^- concentrations in East Asia (15% increases for 40% NH_3 reductions) are much larger than the increases in the other three regions (2-6%). All these differences between East Asia and the other three regions reflect the larger abundance of NH_4NO_3 in SIA over East Asia. This is demonstrated in Fig. S6 which shows that the contribution of fine NO_3^- to $\text{PM}_{2.5}$ in the baseline is greatest in East Asia (19%, $5.21 \mu\text{g m}^{-3}$), followed by Euro_Medi (12%, $1.22 \mu\text{g m}^{-3}$), North America (11%, $0.86 \mu\text{g m}^{-3}$), and South Asia (3%, $0.93 \mu\text{g m}^{-3}$). Detailed discussion on regional SIA composition is presented in Sect. 3.2.



285 **Figure 4: Changes in NO_x and fine NO_3^- annual surface concentrations for 20% and 40% emissions reductions in NH_3 , NO_x , and SO_x individually and collectively. Red and green dots in each map locate the minimum and maximum difference, respectively.**

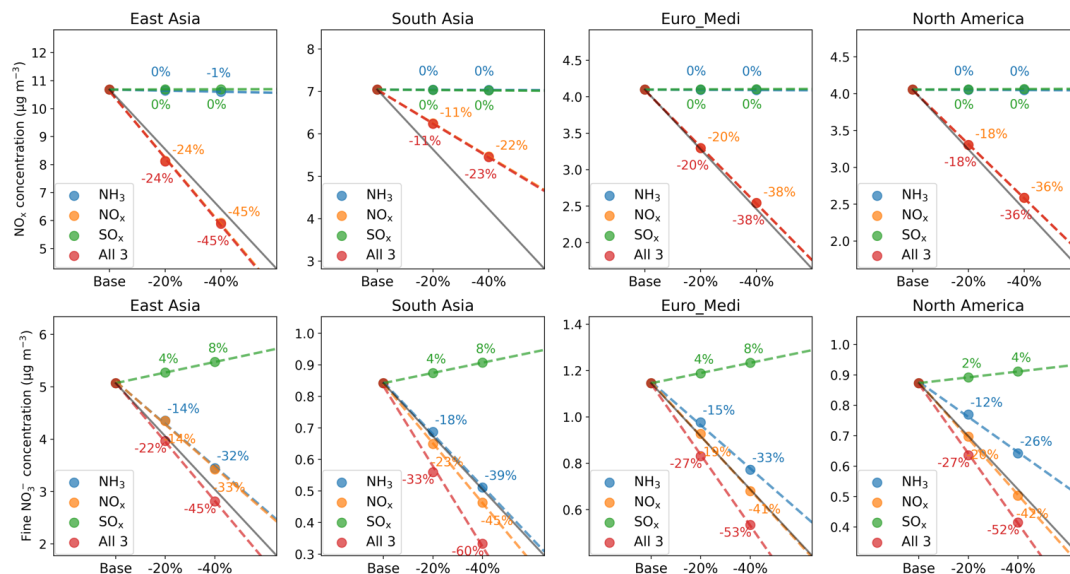


Figure 5: The absolute and relative sensitivities of regionally-averaged annual mean surface concentrations of NO_x (upper row) and fine NO₃⁻ (lower row) to 20% and 40% emissions reductions in NH₃ (blue), NO_x (orange) and SO_x (green) individually, and collectively (red), for the four regions defined in Fig. 1. The solid grey line in each panel illustrates the one-to-one relative response to emissions reductions, whilst the coloured dashed lines are the linear regressions through each set of three model simulations and illustrate the actual responses to emissions reductions of a given precursor. The numbers show the corresponding relative responses to each emissions reduction (with respect to baseline).

290

295 3.1.3 OXS

Figure 6 shows the global variation in the sensitivities of SO₂ and SO₄²⁻ annual mean surface concentrations to 20% and 40% emissions reductions in NH₃, NO_x, and SO_x individually, and collectively. Figure 7 and Table S4 summarise the sensitivities of the regionally averaged SO₂ and SO₄²⁻ concentrations to the emissions reductions for the four regional domains. Concentrations of SO₂ increase in response to reduced NH₃ emissions particularly over East Asia, South Asia, Europe, and North America. The largest increases in SO₂ resulting from 20% and 40% NH₃ emissions reductions are respectively in Southeast Asia (3.62 µg m⁻³, 9%) and East Asia (8.11 µg m⁻³, 20%) (Fig. 6). The response of secondary SO₄²⁻ concentrations to NH₃ emissions reductions varies substantially across the world. In north-eastern China and Europe, SO₄²⁻ concentrations increase, whilst in southern China, India, and United States they decrease. However, the magnitudes of SO₄²⁻ concentration changes are much smaller than for SO₂. The maximum increases in SO₄²⁻ concentrations (located in southern China) are only 0.37 µg m⁻³ (2%) and 0.89 µg m⁻³ (5%) for 20% and 40% NH₃ emissions reductions, respectively. The maximum decreases in SO₄²⁻ concentrations, in north-eastern China, are 0.62 µg m⁻³ (6%) and 1.30 µg m⁻³ (12%), respectively. Regionally averaged, East Asia exhibits the largest increase in SO₂ for 40% NH₃ emissions reductions (16%) (Fig. 7) followed by North America (14%), South Asia (14%), and Euro_Medi (10%), whereas increases in regional average SO₄²⁻ concentrations are only in the range 0-2%.

300

Figures S3 and 13 show the global variation in the sensitivities to precursor emissions reductions of total deposition of SO₂, and of the wet and dry deposition of all OXS components, respectively. When NH₃ emissions are reduced, SO₂ total deposition decreases over all of East Asia, South Asia, Europe, and North America (Fig. S3); Fig. 13 shows the decrease is driven by reduced SO₂ dry deposition. Several studies have shown that the non-stomatal canopy uptake resistance of SO₂ (the inverse of the SO₂ dry deposition velocity) is positively correlated to the molar ‘acidity ratio’ $a_{SN} = \frac{[SO_2]}{[NH_3]}$ (Smith et al., 2000; Erisman et al., 2001; Fowler et al., 2009; Massad et al., 2010), a process that is included in the EMEP MSC-W model (Simpson

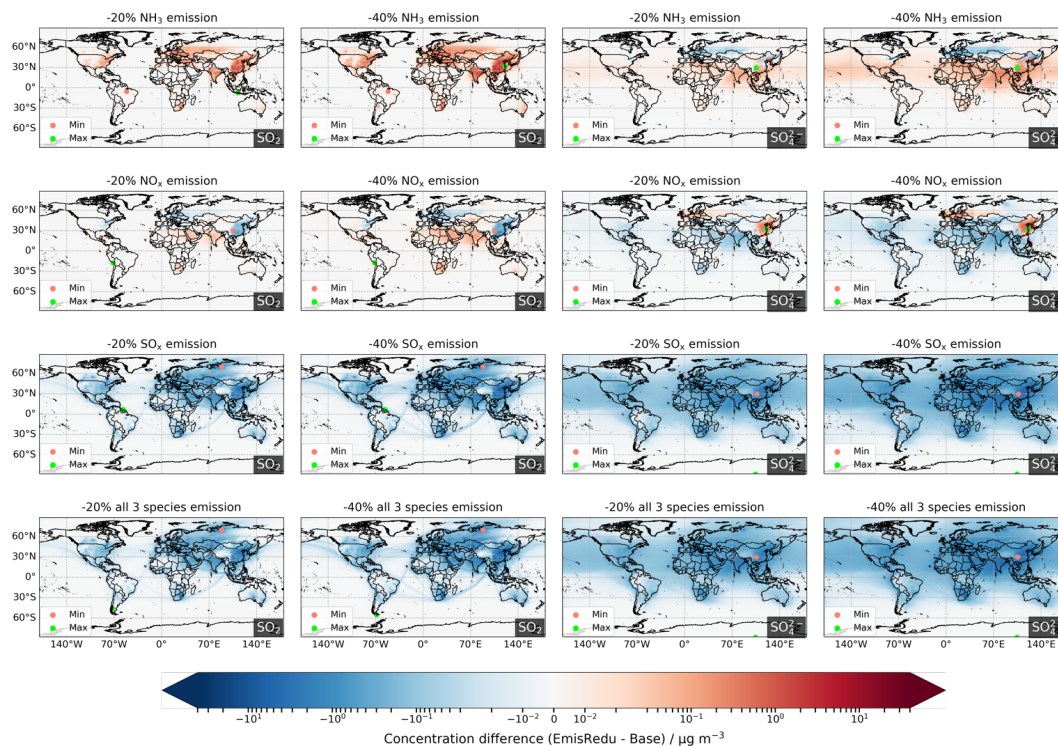
305



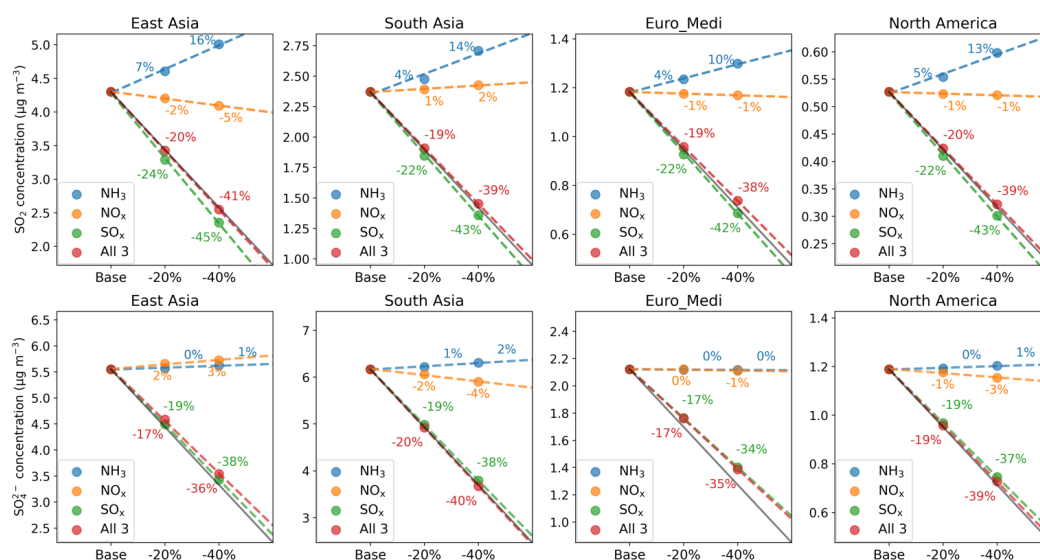
et al., 2012). Reduced NH_3 concentrations therefore increase the acidity ratio and hence decrease the rate of SO_2 dry deposition and increase the SO_2 surface concentrations in those regions where this effect is significant. The SO_4^{2-} responses to NH_3 emissions reductions are related to changes in atmospheric acidity as well. The aqueous-phase oxidation of SO_2 by O_3 , which is one of the major pathways for SO_4^{2-} production, is significantly pH dependent. In general, the oxidation rate decreases with decreased pH (Penkett et al., 1979; Maahs, 1983; Liang and Jacobson, 1999; Hattori et al., 2021), a process that is incorporated into the EMEP MSC-W model (Simpson et al., 2012). As pointed out by Ge et al. (2022), Europe and north-eastern China are much less ammonia-rich than India, which means that 20% and 40% NH_3 emissions reductions are substantial enough to decrease the pH in the former two regions, leading to decreases in SO_4^{2-} production. However, given that SO_2 levels increase and that there are still other effective oxidation pathways (e.g., OH, H_2O_2) which are independent of pH (McArdle and Hoffmann, 1983; Hoffmann, 1986; Seinfeld and Pandis, 2016), the decreases in SO_4^{2-} concentrations in Europe and north-eastern China due to NH_3 emissions reductions are very small anyway. In contrast, since India is so ammonia-rich, even 40% reductions in NH_3 emissions do not significantly alter the pH in this region. As a result, SO_4^{2-} concentrations in India increase slightly due to the higher availability of its precursor SO_2 .

The impacts of NO_x emissions reductions on SO_2 concentrations show inverse trends in different regions (Fig 7), which reflects regional differences in atmospheric oxidation chemistry. The decreased SO_2 concentrations (maximum reduction: $1.72 \mu\text{g m}^{-3}$, 6%) in eastern China, Europe, and north-eastern United States (Fig. 6) can be explained by the enhanced O_3 concentrations in these regions arising from the reduced $\text{NO} + \text{O}_3$ reaction in these high NO_x regions (Fig. S3). As a result, SO_2 is more readily oxidised to SO_4^{2-} , leading to increased SO_4^{2-} concentrations (maximum increase for 40% NO_x emissions reductions: $1.59 \mu\text{g m}^{-3}$ (10%)) in these regions. This positive response of SO_4^{2-} to NO_x emissions reductions is also reported in regional studies (Botha et al., 1994; Li et al., 2006; Sheng et al., 2018; Fang et al., 2019; Ge et al., 2021a). In contrast, India, north-eastern Africa, and southern Africa show increased SO_2 (maximum increase: $0.29 \mu\text{g m}^{-3}$, 1%) but decreased SO_4^{2-} concentrations (maximum decrease: $0.73 \mu\text{g m}^{-3}$, 9%) as NO_x emissions reduce, which can be explained by the parallel decrease in O_3 concentrations in these regions (Fig. S3). However, these concentration changes are very localised and, from a regional average perspective, are relatively small compared to the extent of emissions reductions applied. For example, in East Asia, the region with the largest response, there is only a 5% decrease in regional average SO_2 concentration (Fig. 7), and 3% increase in SO_4^{2-} concentration, for a 40% reduction in NO_x emissions. For other regions, the SO_2 and SO_4^{2-} regional average concentration changes are even smaller (from -4% to 2%). The global average sensitivities of SO_2 and SO_4^{2-} annual mean concentrations to 20% and 40% NO_x emissions reductions are only in the range 0-2% (Table S4).

Under reductions of SO_x emissions (and of all 3 precursors together), both SO_2 and SO_4^{2-} show almost one-to-one reductions, indicating that SO_x emissions reductions are crucial for reducing both primary and secondary OXS pollutants and, in the case of reductions of all 3 precursors simultaneously, readily sufficient to dominate over any tendency for NH_3 and NO_x emissions reductions to increase OXS species concentrations. A 40% reduction in SO_x emissions leads to a maximum SO_2 decrease of $39.8 \mu\text{g m}^{-3}$ (40%), in northern Russia, and a maximum SO_4^{2-} decrease of $7.70 \mu\text{g m}^{-3}$ (39%), in south-eastern China (Fig. 6). For the four regions, average SO_2 concentrations decrease by 22-24% and 42-45%, and SO_4^{2-} concentrations decrease by 17-19% and 34-38%, in response to 20% and 40% SO_x emissions reductions respectively (Fig. 7). For the 20% and 40% reductions in all 3 precursors together, regionally averaged SO_2 decrease by 19-20% and 38-41% respectively, and regionally averaged SO_4^{2-} decrease by 17-20% and 35-40% respectively.



355 **Figure 6:** Changes in SO_2 and SO_4^{2-} annual surface concentrations for 20% and 40% emissions reductions in NH_3 , NO_x , and SO_x individually and collectively. Red and green dots in each map locate the minimum and maximum difference, respectively.



360 **Figure 7:** The absolute and relative sensitivities of regionally-averaged annual mean surface concentrations of SO_2 (upper row) and SO_4^{2-} (lower row) to 20% and 40% emissions reductions in NH_3 (blue), NO_x (orange) and SO_x (green) individually, and collectively (red), for the four regions defined in Fig. 1. The solid grey line in each panel illustrates the one-to-one relative response to emissions reductions, whilst the coloured dashed lines are the linear regressions through each set of three model simulations and illustrate the actual responses to emissions reductions of a given precursor. The numbers show the corresponding relative responses to each emissions reduction (with respect to baseline).

365



3.2 Sensitivity of PM_{2.5} concentrations

Figure 8 shows the global distribution of the dominant sensitivity of PM_{2.5} towards a 40% reduction in NH₃, NO_x, or SO_x emissions individually. An annual mean PM_{2.5} concentration threshold of 5 µg m⁻³ has been applied in order to focus attention away from the most remote areas where PM_{2.5} concentrations in the baseline simulation are already below the latest WHO PM_{2.5} air quality guideline (AQG) (WHO, 2021).

The principal observation from Fig. 8 is that the sensitivity of PM_{2.5} to reductions in emissions of individual precursors is highly geographically variable. SO_x-sensitive regimes are found in Southeast Asia, South Asia, Africa, and Central America. NO_x-sensitive regimes are observed in south-eastern China, France, Germany, most eastern European countries, central and eastern United States, and northern and central parts of South America. Only a few small regions are NH₃ sensitive: these include eastern coastal areas around China, the UK and its surrounding seas, southern Scandinavia, and western Russia. The difference in PM_{2.5} sensitivity between northern Europe and the rest of Europe demonstrates that NH₃ has become the limiting factor for SIA formation in northern Europe. This greater leverage of NH₃ emissions on PM_{2.5} mitigation in this region is due to the effective emissions controls on all SIA precursor emissions here (see also Sect. 4 discussion) (Tørseth et al., 2012; AQEG, 2015; Vieno et al., 2016; Ciarelli et al., 2019; Theobald et al., 2019). In contrast, South Asia is so ammonia-rich that reducing NH₃ concentrations has little impact on PM_{2.5} (Ge et al., 2022). The situation in northern Europe exemplifies what to expect in terms of future policy making for the rest of the world.

Many marine areas are characterised as SO_x sensitive but for a different reason than the SO_x sensitivity in South Asia. In the marine areas, sulfate aerosol derived from oceanic emissions of DMS rather than from anthropogenic emissions is the major contributor to PM_{2.5} (Quinn and Bates, 2011; Hoffmann et al., 2016; Novak et al., 2022).

385

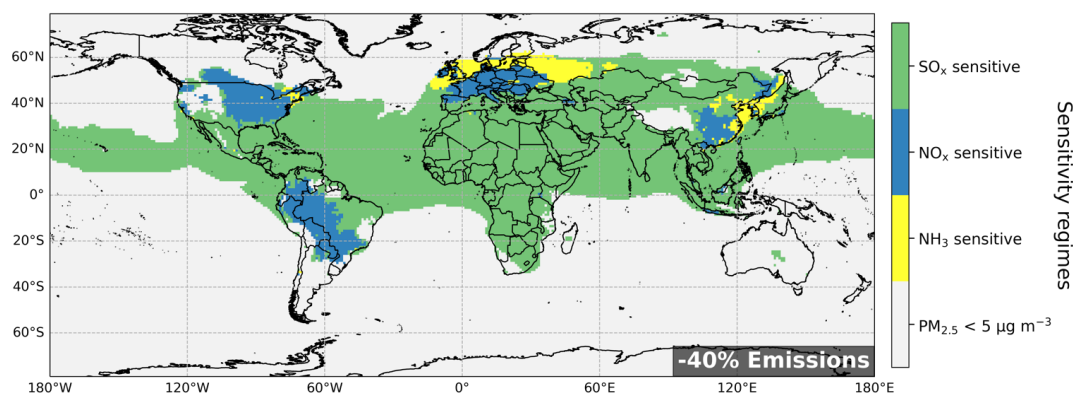


Figure 8: Spatial variation in sensitivity regime of PM_{2.5} mitigation based on data from 40% individual reductions in emissions of NH₃, NO_x, or SO_x. The regime is defined according to the precursor that yields the greatest decreases in grid PM_{2.5} concentration: NH₃ sensitive (yellow), NO_x sensitive (blue), SO_x sensitive (green). Model grids with baseline annual mean PM_{2.5} concentrations <5 µg m⁻³ are masked out.

390

Detailed examination of the magnitudes of the PM_{2.5} sensitivities in each location to each precursor (rather than just their ranking) reveals more complicated regional characteristics. Figure 9 shows the spatial variabilities in PM_{2.5} sensitivities to 40% reductions in emissions of NH₃, NO_x, and SO_x individually, and collectively, for the four world regions. The regionally averaged PM_{2.5} sensitivities are summarised in Fig. 10 and Table S5. PM_{2.5} concentrations in East Asia show comparable sensitivities to individual emissions reductions in NH₃, NO_x, and SO_x, with the impacts of NH₃ and NO_x emissions reductions being more concentrated in continental areas than those for SO_x emissions reductions (Fig. 9). A 40% reduction in NO_x emissions yields a maximum decrease in PM_{2.5} of 11.5 µg m⁻³ (12%) over southern China, while 40% reductions in NH₃ and

395



SO_x yield slightly smaller maximum PM_{2.5} decreases of 8.51 μg m⁻³ (10%) and 8.78 μg m⁻³ (9%), respectively. The regional
400 average sensitivities of PM_{2.5} concentrations in East Asia to 40% reductions in individual precursors are ~8% (Fig. 10).

In contrast, PM_{2.5} concentrations in South Asia only show significant responses to SO_x emissions reductions, whilst NH₃
emissions reductions have little effect, which is consistent with our previous finding that South Asia has the most ammonia-
rich chemical climate for SIA formation (Ge et al., 2022). The dominant proportion of (NH₄)₂SO₄ in SIA compared to NH₄NO₃
in South Asia (Fig. S6) also explains the small sensitivity of PM_{2.5} in this region to NO_x emissions reductions. The maximum
405 PM_{2.5} decrease (7.02 μg m⁻³, 9%) for 40% SO_x emissions reductions is more than three times larger than the maximum PM_{2.5}
decrease (2.20 μg m⁻³, 4%) for 40% NH₃ emissions reductions. The decreases in regionally averaged PM_{2.5} concentrations in
South Asia in response to 40% reductions in emissions of individual precursors are in the order 10% for SO_x, 3% for NO_x, and
1% for NH₃.

In the Euro_Medi region, PM_{2.5} sensitivities vary from north to south. Northern and central Europe is most sensitive to
410 NH₃ and NO_x emissions reductions, for which the maximum decrease in PM_{2.5} is ~2.6 μg m⁻³ (16%) for 40% reductions, while
the Mediterranean is more sensitive to SO_x emissions reductions, for which the maximum decrease in PM_{2.5} is 2.98 μg m⁻³
(12%) for 40% reductions. Regionally averaged, however, the PM_{2.5} concentrations in Euro_Medi show comparable
sensitivities to the three precursors with decreases in the range 5-8% for 40% emissions reductions in individual precursors.

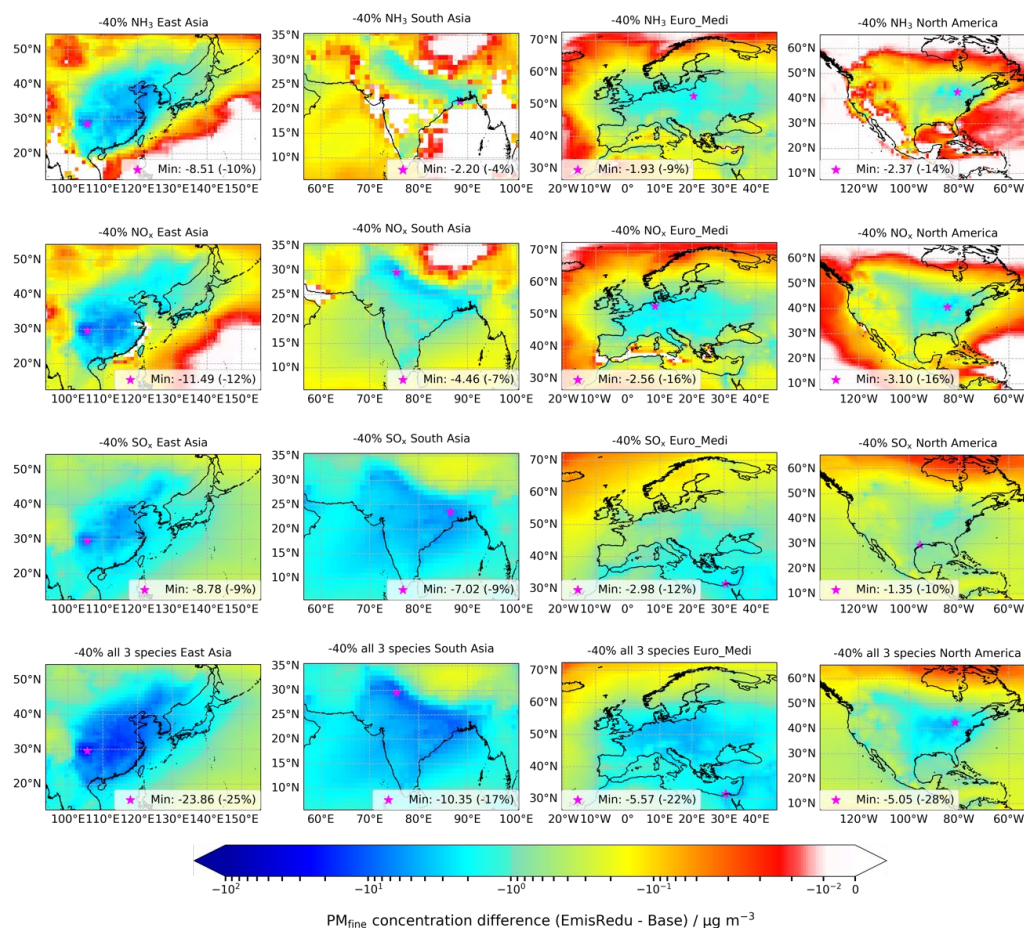
Over North America, the eastern US shows larger sensitivities of PM_{2.5} to all emissions reduction scenarios than the
415 western US, and reductions in NO_x emissions yield larger decreases in PM_{2.5} than reductions in SO_x and NH₃ emissions. The
maximum decrease in PM_{2.5} derived from 40% reductions in NO_x emissions is 3.10 μg m⁻³ (16%); for 40% reductions in NH₃
and SO_x emissions the maximum PM_{2.5} decreases are 2.37 μg m⁻³ (14%) and 1.35 μg m⁻³ (10%) respectively. The regional
average sensitivities of PM_{2.5} concentrations in North America to 40% reductions in emissions of individual precursors
decreases in a slightly different order: NO_x (8%), SO_x (7%), and NH₃ (4%).

Figure 10 shows that 20% emissions reductions in any precursor lead to decreases in regionally averaged PM_{2.5}
420 concentrations, although the PM_{2.5} sensitivities vary substantially with precursor and region. Given the non-one-to-one
chemical responses of SIA components to reductions in emissions in individual precursors discussed in Sect. 3.1, even 20%
reductions appear substantial enough to ensure that decreased SIA formation due to decreased precursor emissions dominates
over any disbenefits to SIA formation from, for example, increases in oxidant levels induced by NO_x emissions reductions.
425 For instance, 20% reductions in NO_x emissions still cause a decrease of 0.77 μg m⁻³ (3%) in regional average PM_{2.5} in East
Asia, despite increasing regional average SO₄²⁻ by 0.10 μg m⁻³ (2%) because it decreases regional average NH₄⁺ and fine NO₃⁻
by greater amounts (0.17 μg m⁻³ (5%) and 0.72 μg m⁻³ (14%) respectively). Similarly, 20% reductions in SO_x emissions
decrease regional average PM_{2.5} in East Asia by 1.15 μg m⁻³ (4%) because the decreases in SO₄²⁻ (1.06 μg m⁻³, 19%) and NH₄⁺
(0.32 μg m⁻³, 9%) caused by reduced (NH₄)₂SO₄ formation are larger than the increase in fine NO₃⁻ (0.20 μg m⁻³, 4%) due to
430 elevated NH₄NO₃ formation. On the other hand, the mitigation of PM_{2.5} by reducing emissions of all 3 precursors together is
impacted by these non-one-to-one chemical responses as well, which causes the net decrease in regional average PM_{2.5} derived
from reductions in all 3 precursors to be smaller than the sum of individual PM_{2.5} decreases derived from reductions in
emissions of precursors individually. For example, 40% reductions in NH₃, NO_x and SO_x emissions individually decrease
regional average PM_{2.5} in East Asia by 2.03 μg m⁻³ (7%), 1.89 μg m⁻³ (7%), and 2.33 μg m⁻³ (8%) respectively (sum of the
435 three: 6.25 μg m⁻³), while the decrease in regional average PM_{2.5} derived from 40% reduction in all 3 precursors simultaneously
is 5.59 μg m⁻³ (20%).

The 40% reduction in emissions of all 3 species yields a maximum decrease in PM_{2.5} of 23.9 μg m⁻³ (25%) over East Asia,
followed by 10.4 μg m⁻³ (17%) in South Asia, 5.57 μg m⁻³ (22%) in Euro_Medi, and 5.05 μg m⁻³ (28%) in North America.
The regional average sensitivity of PM_{2.5} concentrations to 20% and 40% reductions in emissions of all 3 species decreases in
440 the order East Asia (10% and 20% for 20% and 40% reductions respectively), Euro_Medi (9% and 17%), North America (8%

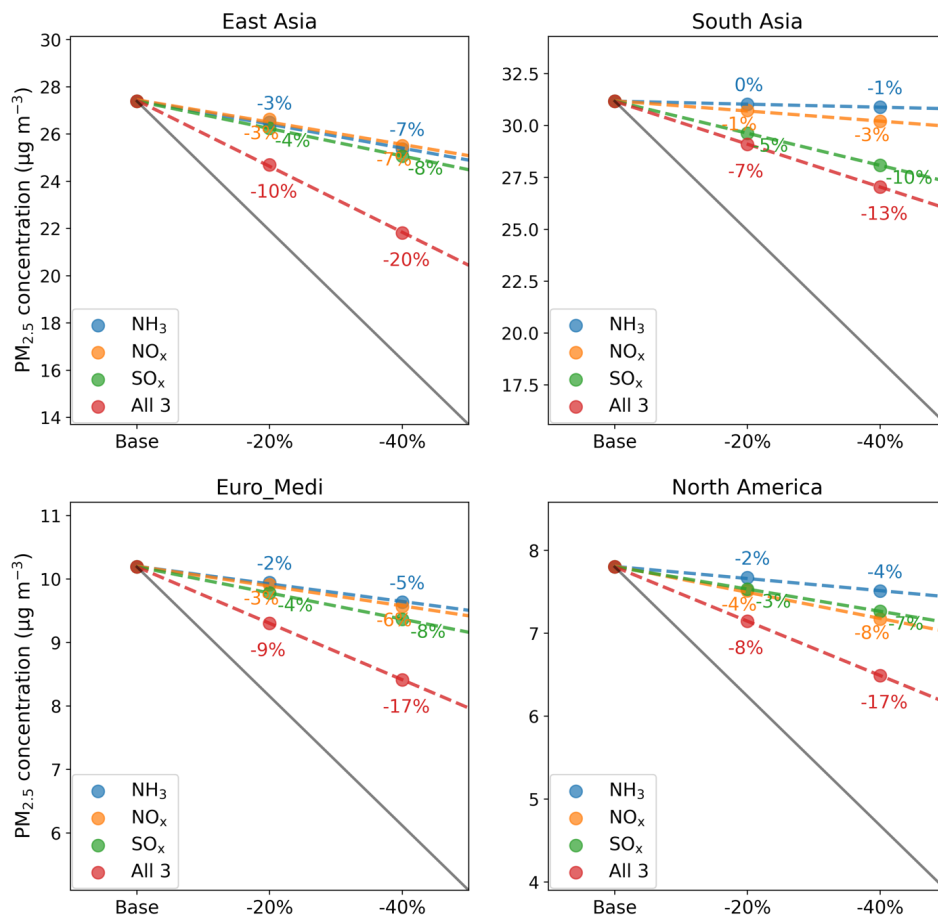


and 17%), and South Asia (7% and 13%). This trend is related to differences in the contribution of SIA to $PM_{2.5}$ in the different regions. Figure S6 shows the mass contributions of individual $PM_{2.5}$ components to the regional average concentration of $PM_{2.5}$ in the baseline and the 40% emissions reductions scenarios. SIA components in the baseline account for over half of $PM_{2.5}$ in East Asia (52%), followed by Euro_Medi (42%), North America (35%), and South Asia (31%), which explains why reductions in emissions of all three SIA precursors are most efficient for the mitigation of $PM_{2.5}$ in East Asia but least efficient in South Asia. In fact, primary $PM_{2.5}$ is the largest contributor to $PM_{2.5}$ in South Asia, so reducing these emissions will be the most efficient way of abating $PM_{2.5}$ pollution in this region. It is noteworthy that in the scenario of 40% reductions in all 3 species, SIA is still the largest contributor to $PM_{2.5}$ in East Asia, while primary $PM_{2.5}$ and Rest (mainly secondary organic aerosol) become the dominant contributors in other regions. Even with 40% reductions in all three SIA precursors, none of the four regions has its regional average $PM_{2.5}$ concentration decreased to below $5 \mu g m^{-3}$. Euro_Medi ($8.4 \mu g m^{-3}$ after 40% reductions) and North America ($6.5 \mu g m^{-3}$) are the closest, whilst East Asia ($21.8 \mu g m^{-3}$) and South Asia ($27.0 \mu g m^{-3}$) are still far away from achieving the latest WHO AQG for $PM_{2.5}$. Therefore, reductions in emissions of primary $PM_{2.5}$ and in VOCs are also required to achieve further $PM_{2.5}$ reductions in all regions, or even greater reductions in SIA precursors than simulated here.



455

Figure 9: Changes in $PM_{2.5}$ annual mean surface concentrations for 40% emissions reductions in NH_3 , NO_x , and SO_x individually and collectively. The pink star in each map locates the minimum difference within each region.



460 **Figure 10: The absolute and relative sensitivities of regionally-averaged annual mean surface concentrations of PM_{2.5} to 20% and 40% emissions reductions in NH₃ (blue), NO_x (orange) and SO_x (green) individually, and collectively (red), for the four regions defined in Fig. 1. The solid grey line in each panel illustrates the one-to-one relative response to emissions reductions, whilst the coloured dashed lines are the linear regressions through each set of three model simulations and illustrate the actual responses to emissions reductions of a given precursor. The numbers show the corresponding relative responses to each emissions reduction (with respect to baseline).**

465

3.3 Sensitivity of N_r and S_r deposition

The impacts of reductions in emissions of NH₃, NO_x and SO_x on total amounts of N and S deposition are straightforward because these must match the emissions mass changes in N and S. However, the relative amounts and spatial pattern of the individual components of N and S deposition are impacted.

470

Figure 11 shows the spatial variations in the sensitivities of the wet and dry deposition of the RDN components NH₃ and NH₄⁺ to 40% reductions in global emissions of NH₃, NO_x, SO_x individually, and collectively. Figure 12 shows similar for deposition of the OXN components NO_x, HNO₃, TNO₃⁻ (total NO₃⁻; the sum of fine and coarse NO₃⁻) and Rest (the sum of other oxidized N species). Both wet and dry deposition of NH₃ show negative responses to emissions reductions in NH₃ and all 3 precursors together, but positive responses to emissions reductions in NO_x and SO_x, which is consistent with the responses of surface NH₃ concentrations to these emissions reductions (Sect. 3.1.1). This is because reduced NO_x and SO_x emissions lead to decreased concentrations of acidic species in the atmosphere, resulting in more NH₃ remaining in the gas phase and

475



greater NH_3 deposition over continents. In contrast, global NH_4^+ wet and dry deposition decreases in all emissions reduction scenarios, which is also in line with the decreased NH_4^+ concentrations in all scenarios.

480 The changes in deposition of the OXN components to emissions reductions are more complicated (Fig. 12). The two species with the largest variation in deposition across the emissions reduction scenarios are HNO_3 and TNO_3^- , which is due to their large contributions to total OXN deposition in most world regions (Ge et al., 2022). For reductions in emissions of NO_x and all 3 species, all OXN deposition components show clear decreasing trends due to the strong reduction in their precursor emissions.

485 In response to NH_3 emissions reductions, Fig. 12 shows that HNO_3 wet and dry deposition increases in eastern China, northern India, Europe, and eastern North America, whereas the wet and dry deposition of TNO_3^- decreases in these regions. Further examination of fine and coarse NO_3^- deposition differences in Fig. S7 shows that the decrease in TNO_3^- deposition is driven by the decrease in fine NO_3^- wet and dry deposition, while coarse NO_3^- wet and dry deposition in the four regions actually increases. The reduction in NH_3 emissions decreases NH_4NO_3 formation and therefore liberates more HNO_3 ; as a result, more OXN deposits in the form of HNO_3 rather than NO_3^- in these regions. In contrast, impacts of SO_x emissions
490 reductions on HNO_3 and TNO_3^- deposition are the opposite of impacts of NH_3 emissions reductions. As discussed in Sect. 3.1.2, decreased SO_4^{2-} concentrations promote the formation of NH_4NO_3 , which results in decreased wet and dry deposition of HNO_3 and consequently increased TNO_3^- deposition (driven by increased fine NO_3^- deposition, Fig. S7) in eastern China, northern India, Europe, and eastern North America.

495 Compared to HNO_3 and TNO_3^- , the responses of NO_x and Rest OXN deposition to reductions in NH_3 and SO_x emissions are considerably smaller. For instance, the maximum increases in HNO_3 wet and dry deposition in response to 40% NH_3 emissions reductions are 328 mgN m^{-2} (85%) and 248 mgN m^{-2} (48%) respectively, whereas the maximum increases in Rest OXN wet and dry deposition are only 1.35 mgN m^{-2} (4%) and 1.64 mgN m^{-2} (4%) respectively. Also, in the 40% NH_3 emissions reduction scenario, the maximum decreases in TNO_3^- wet and dry deposition are 359 mgN m^{-2} (25%) and 175 mgN m^{-2} (28%) respectively, whereas the maximum decreases in NO_x dry deposition are only 4.22 mgN m^{-2} (1%).

500

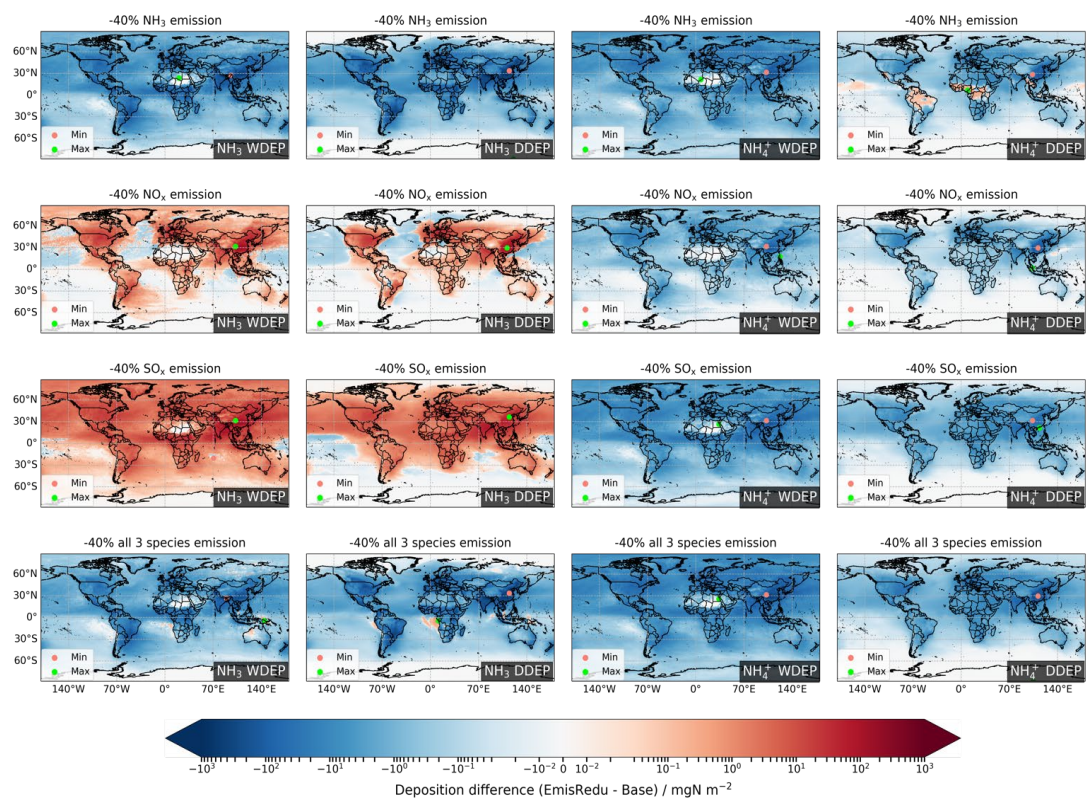


Figure 11: Changes in wet (WDEP) and dry deposition (DDEP) of NH₃ and NH₄⁺ for 40% emissions reductions in NH₃, NO_x, and SO_x individually and collectively. Red and green dots in each map locate the minimum and maximum difference, respectively.

505

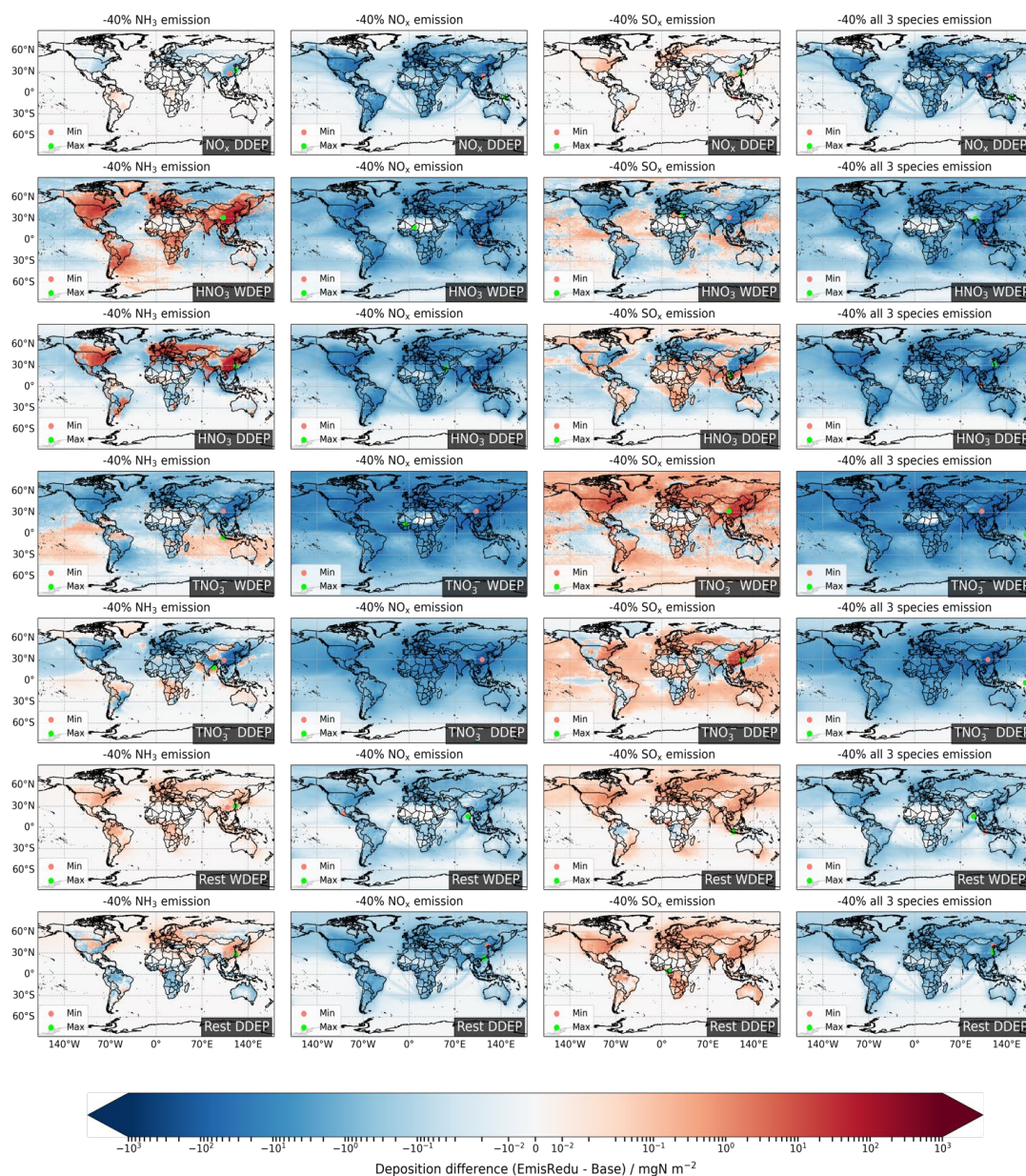


Figure 12: Changes in wet (WDEP) and dry deposition (DDEP) of NO_x, HNO₃, TNO₃⁻ (fine + coarse NO₃⁻), and Rest OXN species for 40% emissions reductions in NH₃, NO_x, and SO_x individually and collectively. Red and green dots in each map locate the minimum and maximum difference, respectively.

510

The spatial variations in the sensitivities of SO₂ and SO₄²⁻ wet and dry deposition to the precursor emissions reductions are shown in Fig. 13. Increased SO₂ wet deposition is observed globally in response to NH₃ emissions reductions, whilst SO₂ dry deposition decreases over the continents but increases over the oceans. The non-stomatal canopy resistance of SO₂ is positively correlated to the molar acidity ratio a_{SN} (Smith et al., 2000; Erisman et al., 2001; Fowler et al., 2009; Massad et al., 2010; Simpson et al., 2012). Reductions in NH₃ emissions increase the a_{SN} , which therefore increases the canopy resistance

515

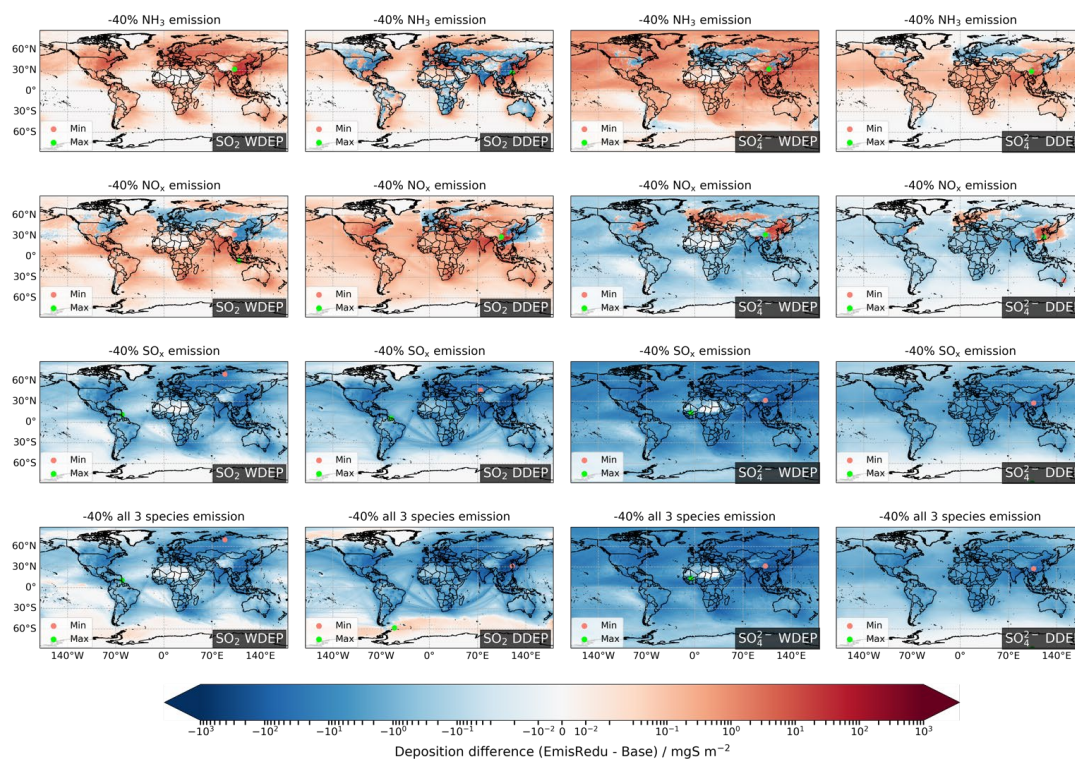


of SO₂ and decreases SO₂ dry deposition over the continents. The 40% reduction in NH₃ emissions yields a global maximum increase in SO₂ wet deposition of 131 mgS m⁻² (44%), and a maximum decrease in SO₂ dry deposition of 600 mgS m⁻² (24%). The overall effect of increased SO₂ wet deposition and decreased SO₂ dry deposition is a decreased SO₂ total deposition over populated continents (where NH₃ emissions are high) and increased SO₂ total deposition over oceans (Fig. S4). The maximum decrease of SO₂ total deposition located in southern China is 586 mgS m⁻² (18%) for 40% NH₃ reduction.

The sensitivity of total deposition of SO₄²⁻ to NH₃ emissions reductions (Fig. S5) follows the trend in the sensitivity of SO₄²⁻ concentrations (Sect. 3.1.3). The responses of wet and dry deposition of SO₄²⁻ to NH₃ emissions reductions are similar (Fig. 13). In general, decreased wet and dry SO₄²⁻ deposition appears over Europe, north-eastern China, and north-eastern US, while increased wet and dry deposition occurs in the rest of the world. As also for their concentration sensitivities, the magnitudes of the SO₄²⁻ deposition responses are much smaller than for SO₂. For 40% NH₃ emissions reduction, the maximum decrease of SO₄²⁻ total deposition is 42 mgS m⁻² (9%), which is an order of magnitude smaller than that of SO₂ total deposition.

For NO_x emissions reductions, both wet and dry deposition of SO₂ generally show decreases in eastern China, Europe, and north-eastern US but increases in the rest of the world, which is contrary to the responses of SO₄²⁻ wet and dry deposition. This is related to enhanced chemical conversion of SO₂ to SO₄²⁻ due to increased atmospheric oxidizing capacity over eastern China, Europe, and north-eastern US (details in Sect. 3.1.3). The maximum decrease in SO₂ wet and dry deposition in response to 40% reductions in NO_x emissions is ~65 mgS m⁻², while the maximum increase in SO₄²⁻ wet and dry deposition is ~50 mgS m⁻².

For reductions in SO_x and in all 3 precursors collectively, decreased wet and dry deposition of SO₂ and SO₄²⁻ is observed globally and the 40% reductions in these two scenarios yield similar global maximum decreases in SO₂ deposition (wet: ~937 mgS m⁻², 41%; dry: ~1338 mgS m⁻², 43%) and SO₄²⁻ deposition (wet: ~828 mgS m⁻², 38%; dry: ~150 mgS m⁻², 39%).



540 **Figure 13: Changes in wet (WDEP) and dry deposition (DDEP) of SO₂ and SO₄²⁻ for 40% emissions reductions in NH₃, NO_x, and SO_x individually and collectively. Red and green dots in each map locate the minimum and maximum difference, respectively.**



Figure 14 shows the differences of regional total deposition of individual species between baseline and the 40% emissions reduction scenarios. The regional total RDN, OXN and OXS deposition and the contributions of individual components are listed in Table S6 and S7. As expected, the responses of regional total RDN, OXN and OXS deposition are essentially linear through 20% and 40% reductions in their corresponding precursor, and largely insensitive to reductions in the other precursors, although there are slight differences between regions. For example, 20% and 40% reductions in NH_3 emissions respectively yield 20-21% and 39-41% decreases in total deposition of RDN in the four regions, whilst having no effect on regional total OXN and OXS deposition. The contributions of different deposition components do, however, vary with emission changes and the different lifetimes of the deposition components contribute to the small variabilities in responses of total RDN, OXN and OXS deposition to emissions reductions via differences in the transport through the regional boundaries.

A 40% reduction in NH_3 emissions produces a decrease of 3.58 TgN yr^{-1} (51% of regional total deposition of the same species in baseline; similarly, hereinafter) in NH_3 total deposition and 1.16 TgN yr^{-1} (24%) in NH_4^+ total deposition over East Asia (Fig. 14), which causes the contribution of NH_3 to RDN deposition to decrease from 59% (baseline) to 47% (after 40% NH_3 reduction). In other regions, reductions in NH_3 emissions also decrease NH_3 deposition more effectively than NH_4^+ deposition. Also in East Asia, a 40% NH_3 emissions reduction increases HNO_3 deposition by 0.61 TgN yr^{-1} (20%) and SO_4^{2-} deposition by 0.06 TgS yr^{-1} (2%) but decreases TNO_3^- deposition by 0.55 TgN yr^{-1} (14%) and SO_2 deposition by 0.12 TgS yr^{-1} (3%). As a result, the contribution of HNO_3 deposition to total OXN deposition increases from 30% to 37%, corresponding to a decrease in TNO_3^- contribution from 54% to 47%, whereas changes in contributions of SO_2 and SO_4^{2-} to OXS deposition are very small (Table S7). In other world regions, such changes in total deposition of HNO_3 , TNO_3^- , SO_2 , and SO_4^{2-} derived from NH_3 emissions reductions are similar but of smaller magnitude.

For 40% NO_x emissions reductions, TNO_3^- deposition shows the largest decrease in East Asia (1.57 TgN yr^{-1} , 35%), South Asia (0.44 TgN yr^{-1} , 26%), and Euro_Medi (0.71 TgN yr^{-1} , 37%), whilst HNO_3 deposition shows the largest decrease in North America (0.56 TgN yr^{-1} , 40%). In contrast, the sensitivities of NO_x dry deposition to NO_x emissions reductions are very small. The contributions of individual OXN deposition components remain fairly constant in all regions. Furthermore, East Asia, Euro_Medi, and North America show a 5% increase in the contribution of NH_3 deposition to total RDN deposition and a corresponding 5% decrease in NH_4^+ contribution for 40% NO_x emissions reductions, which reflects a small shifting of gas-aerosol partitioning for RDN as well. This kind of contribution change in RDN deposition is 2% for South Asia. The impacts of NO_x emissions reductions on OXS deposition compositions are very small.

The 40% reductions in SO_x emissions yield 3.24 TgS yr^{-1} (39%), 1.07 TgS yr^{-1} (38%), 1.17 TgS yr^{-1} (33%), and 0.78 (37%) TgS yr^{-1} decreases in OXS deposition over East Asia, South Asia, Euro_Medi, and North America respectively. SO_x emissions reductions cause larger decreases in SO_2 deposition than in SO_4^{2-} deposition in East Asia and Euro_Medi, while SO_2 and SO_4^{2-} deposition in South Asia and North America show similar sensitivities. This is associated with slightly greater proportions of SO_2 (56-58%) to OXS deposition in the former regions than in the latter regions, and that these proportions are not affected by SO_x emissions reductions (Table S7). NH_3 and NH_4^+ deposition is moderately sensitive to SO_x emissions reductions in the four regions. An increase of 0.75 TgN yr^{-1} (11%) in NH_3 total deposition and a decrease of 0.71 TgN yr^{-1} (14%) in NH_4^+ total deposition for 40% reductions in SO_x emissions is observed over East Asia. For South Asia, Euro_Medi, and North America, the increases in NH_3 total deposition due to 40% SO_x reductions are 0.51 TgN yr^{-1} (12%), 0.25 TgN yr^{-1} (11%), and 0.23 TgN yr^{-1} (12%) respectively. This is because reduced SO_x emissions lead to reductions in $(\text{NH}_4)_2\text{SO}_4$ formation which then cause increased NH_3 but decreased NH_4^+ concentrations. Another side effect of SO_x emissions reductions in East Asia is a slight decrease in HNO_3 deposition (0.25 TgN yr^{-1} , 10%) and an equivalent increase in TNO_3^- deposition (0.21 TgN yr^{-1} , 5%). The equivalent deposition changes are considerably smaller in the other three regions, which again indicates a larger amount of NH_4NO_3 pollution in East Asia than other regions.

For collective reductions in emissions of all precursors, the changes in deposition of each species reflect net effects of individual reductions in emissions of NH_3 , NO_x , and SO_x . For instance, Fig. 14 shows that the decrease in NH_3 deposition in



East Asia derived from 40% reduction in emissions of all 3 species (2.58 TgN yr^{-1} , 36%) is smaller than that from individual
 585 NH_3 emissions reduction (3.58 TgN yr^{-1} , 51%) due to the compensating effects of simultaneous NO_x and SO_x emissions
 reductions in the former scenario. In contrast, the decrease in NH_4^+ deposition in East Asia for 40% emissions reductions in
 all 3 species (2.11 TgN yr^{-1} , 43%) is almost double that from individual NH_3 emissions reduction scenario (1.16 TgN yr^{-1} ,
 24%). The variations in chemical forms of RDN, OXN, and OXS deposition affect where they deposit as well since N_r and S_r
 590 species have different lifetimes and a shorter lifetime causes a more localised deposition. Many studies show that NH_3 and
 HNO_3 have shorter lifetimes than NH_4^+ and NO_3^- (Xu and Penner, 2012; Hauglustaine et al., 2014; Bian et al., 2017; Ge et al.,
 2022). The abatement of total N (TN = RDN + OXN) and S deposition within a certain region is partially offset by this more
 localised deposition pattern especially in South Asia and Euro_Medi. The 40% reductions in all 3 species emissions yield a
 34% (2.93 TgN yr^{-1}) decrease in regional TN deposition in South Asia, and a 34% (1.18 TgS yr^{-1}) decrease in regional OXS
 595 locally.

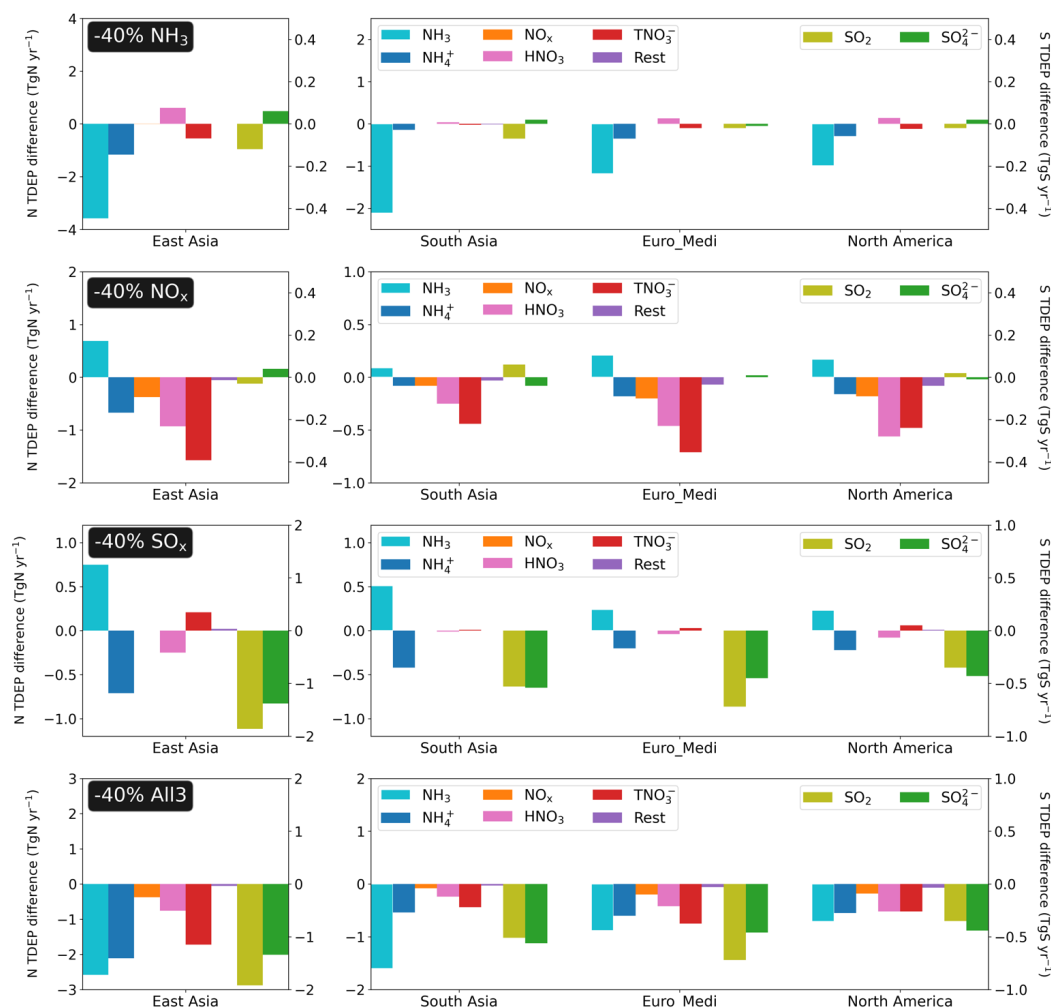


Figure 14: The absolute sensitivities (Emission Reduction - Baseline) of regional total deposition (wet + dry) of NH_3 , NH_4^+ , NO_x , HNO_3 , TNO_3^- (fine + coarse NO_3^-), SO_2 and SO_4^{2-} to 40% emissions reductions in NH_3 (top row), NO_x (2nd row) and SO_x (3rd row) individually, and collectively (bottom row), for the four regions defined in Fig. 1. The left-hand y axis in each panel is for RDN and OXN species, while the right-hand y axis is for OXS species.

600



4 Discussion

We use global model simulations for 8 emissions reduction scenarios to investigate the geographical variation in the effectiveness of mitigation of N_r , S_r , and $PM_{2.5}$ pollution to SIA precursor gas emissions reductions. Although the EMEP MSC-W ACTM is state-of-the-art and widely used in scientific research and policy development, the analyses presented in this study are based on data from a single model. The accurate representation of relevant chemical and physical processes in the model is crucial for simulations of sensitivities of N_r , S_r and $PM_{2.5}$ to emissions reductions in inorganic precursor gaseous. It is possible that variations in aerosol water content under different relative humidity conditions may impact on the exact mass sensitivities of $PM_{2.5}$. However, the evaluation of surface concentrations and wet deposition of N_r and S_r species from this model configuration for the same year against global measurements from 10 monitoring networks (Ge et al., 2021b) has demonstrated the model's capability to capture the overall spatial variations in annual concentrations of NH_3 , NH_4^+ , NO_2 , HNO_3 , fine NO_3^- , SO_2 and SO_4^{2-} and their wet deposition in East Asia, Southeast Asia, Europe, and North America. The uncertainties in both model and measurement constrains the extent to which the agreement between model and measurement can be used to evaluate a model's performance. However, the sensitivities of global and regional N_r , S_r , and $PM_{2.5}$ to various emissions reductions can only be investigated through modelling experiments, and since most model uncertainties will be similar across a set of simulations with the same model configuration, the modelled changes in concentrations between baseline and an emissions reduction scenario should be robust. Nevertheless, considering the fundamental uncertainties in emissions and model parameterizations, all numbers reported in this work should be considered as having uncertainty, albeit that the latest available global emissions inventory and model version were used to minimize the impacts of these uncertainties.

The simulations of emissions reduction scenarios show that the reduction in emissions of one individual precursor has multiple co-benefits and sometimes small disbenefits on mitigating N_r , S_r , and $PM_{2.5}$ pollution, and these effects are geographically variable. In this work, our discussion focuses on East Asia, South Asia, Euro_Medi, and North America because of the high population density and high N_r and S_r pollution in those regions. The comparison of regional responses to emissions reductions reveals differences in regional oxidation regime, SIA chemistry and deposition pattern which are important processes to consider when designing emissions control policies since transitory increases in $PM_{2.5}$ and some N_r and S_r pollutants could occur as emissions reduction measures are gradually applied.

Globally, reductions in NH_3 emissions are effective for reducing NH_3 concentrations and its wet and dry deposition but considerably less effective at reducing NH_4^+ . This is because most world regions are in an ammonia-rich chemical domain in which reducing NH_3 emissions only has limited effects on mitigating SIA formation (Ge et al. 2022). Other co-benefits of NH_3 emissions reductions include reductions in fine NO_3^- surface concentrations and deposition in East Asia, South Asia, Euro_Medi, and North America because of reduced NH_4NO_3 formation. A notable disbenefit is the increased SO_2 surface concentration and human exposure in these regions which is caused by reduced SO_2 dry deposition. The dry deposition velocity of SO_2 is negatively correlated with the molar acidity ratio a_{SN} which is a model parameterisation derived from long-term deposition measurements (Erismann et al., 2001; Simpson et al., 2012). Reduced NH_3 emissions therefore lead to decreased SO_2 dry deposition.

Similarly, whilst reducing NO_x emissions is of course an effective way of decreasing global concentrations and deposition of OXN species, the degree to which different OXN species are decreased varies across regions. A 40% reduction in NO_x emissions decreases NO_x and fine NO_3^- surface concentrations in East Asia by 45% and 33% respectively, whereas in South Asia this measure has a greater effect on fine NO_3^- (45% decrease) than on NO_x (22% decrease). In Euro_Medi and North America, the 40% NO_x emissions reductions produce similar decreases in regional average NO_x (36-38%) and fine NO_3^- (41-42%) concentrations. These trends are consequent on different regional NO_x oxidation regime and SIA chemistry. The NO_x emissions reductions decrease NO_x surface concentrations, which increases O_3 concentrations in the high NO_x areas of eastern China and western and central Europe and therefore increases the atmospheric oxidizing capacity in these regions. As a result, more SO_2 is oxidized to SO_4^{2-} which leads to decreased SO_2 concentrations and deposition and consequently increased SO_4^{2-}



645 concentrations and deposition in these areas. The enhanced SO_4^{2-} production can partially (or even totally) offset the mass
reduction in $\text{PM}_{2.5}$ caused by reduced NH_4NO_3 formation when reductions in NO_x emissions are not sufficiently high. The
increased oxidant levels will also enhance HNO_3 and NO_3^- production in these regions, but this effect does not compensate for
the reduction in HNO_3 and NO_3^- concentrations due to the reductions in NO_x emissions (at least for 20% and 40% NO_x
650 reductions), so the net effect is globally decreased HNO_3 and NO_3^- . Consequently, reduced HNO_3 and NO_3^- levels caused by
 NO_x emissions reductions lead to less NH_4NO_3 formation, which then results in globally increased NH_3 concentration and
deposition and decreased NH_4^+ concentration and deposition. In contrast, decreased O_3 concentrations in South Asia and North
America in response to NO_x emissions reductions result in less chemical conversion of SO_2 to SO_4^{2-} , which then causes
increased SO_2 and decreased SO_4^{2-} concentrations and deposition. Clappier et al. (2021) and Thunis et al. (2021) showed that
the increased atmospheric oxidizing capacity induced by reductions in NO_x emissions is the reason for increased $\text{PM}_{2.5}$ levels
655 in the Po basin (Italy) especially during wintertime, with increased nitrate, sulfate and SOA concentrations all being closely
related to increased O_3 levels. Balamurugan et al. (2022) reported that reductions in SIA were much smaller than NO_2
emissions reductions during COVID lockdown in Germany, which is because the increased oxidant levels (OH , NO_3 and O_3)
enhanced the formation of sulfate and night-time nitrate which then partially offset the lockdown-induced $\text{PM}_{2.5}$ decreases. Fu
et al. (2020) noted that the increased oxidation of NO_x to HNO_3 due to increased O_3 levels makes winter haze NO_3^- in the
660 North China Plain (NCP) almost insensitive to 30% reductions in emissions of NO_x , while Le et al. (2020) also revealed an
unexpected PM exacerbation caused by unfavourable meteorological conditions and intensified SIA formation due to elevated
 O_3 levels induced by NO_x emissions reductions during COVID lockdown in China.

The greatest effect of SO_x emissions reductions is the direct decrease in global concentrations and deposition of SO_2 and
 SO_4^{2-} , which then induces changes in gas-aerosol partitioning of NH_3 - NH_4^+ and HNO_3 - NO_3^- . As discussed above, the reduction
665 in $(\text{NH}_4)_2\text{SO}_4$ formation frees more gaseous NH_3 and promotes NH_4NO_3 formation, leading to increased concentrations and
deposition of NH_3 and fine NO_3^- in all world regions. Considering that one SO_4^{2-} takes up two NH_3 molecules under ammonia-
rich conditions, but NO_3^- only takes one, the net effect of SO_x emissions reductions still causes globally decreased NH_4^+
concentrations and deposition. Liu et al. (2018) noted a significant increase in annual NH_3 concentrations caused by rapid SO_2
emissions reductions in the NCP. In addition, the shifting of RDN from aerosol-phase NH_4^+ to gaseous NH_3 in response to
670 reduced SO_x emissions also means that RDN pollution becomes more localized because NH_3 has a much shorter lifetime (1.6
days) than NH_4^+ (8.9 days) as it deposits more quickly to land rather than being transported to other regions (Ge et al. 2022).
Utilizing combined measurements and modelling, Leung et al. (2020) found that the reduction in wintertime $\text{PM}_{2.5}$ in the NCP
is buffered by enhanced NH_4NO_3 formation due to decreased SO_4^{2-} concentration liberating free NH_3 , and increased oxidant
levels promoting HNO_3 production, despite SO_2 and NO_x emissions reductions in China. However, it is important to note that
675 $(\text{NH}_4)_2\text{SO}_4$ has greater molecular mass than NH_4NO_3 and hence has larger leverage on $\text{PM}_{2.5}$ mass concentration, which ensures
that the reductions in $\text{PM}_{2.5}$ mass concentrations derived from reduced $(\text{NH}_4)_2\text{SO}_4$ are less readily compensated by increases
in NH_4NO_3 concentrations. This also means that relative changes in the SO_4^{2-} component cause greater mass changes with
respect to $\text{PM}_{2.5}$ air quality objectives (which must be expressed as mass concentration) than do the same relative changes in
the NO_3^- component. The relative changes in the SIA components of $\text{PM}_{2.5}$ expressed as molar concentrations would be
680 different.

The simulations for both 20% and 40% emissions reductions scenarios show that the most effective emissions control for
decreasing regional average $\text{PM}_{2.5}$ concentrations, via an individual component, differs between world regions. $\text{PM}_{2.5}$ in South
Asia is most sensitive to SO_x emissions reductions, and least sensitive to NH_3 emissions reductions, which is because South
Asia is extremely ammonia rich (Ge et al., 2022) so reducing NH_3 has little impact on mitigating SIA. In this study, 40%
685 reductions in SO_x and NH_3 emissions respectively produce 10% and 1% decreases in South Asia regional average $\text{PM}_{2.5}$.
Pozzer et al. (2017) also showed that NH_3 emissions control has negligible impacts on $\text{PM}_{2.5}$ levels in South Asia with a 50%
reduction in NH_3 emissions only reducing annual mean $\text{PM}_{2.5}$ by 2%. The most effective measure to reduce annual mean $\text{PM}_{2.5}$



in North America is reducing NO_x emissions, followed by SO_x and then NH₃. Liao et al. (2008) reported that the reduction in NO_x emissions was most effective for decreasing 24-h mean PM_{2.5} levels for five cities in the US, while Kelly et al. (2021) reported that reducing NO_x emissions was more effective for reducing PM_{2.5} concentrations in the eastern US than SO₂, NH₃, and VOC emissions reductions in both January and July. Tsimpidi et al. (2007, 2008) showed that NO_x emissions reductions were the most effective measure for controlling PM_{2.5} in the eastern US in summer due to the combined effects of lower atmospheric oxidant levels and smaller precursor emissions. Unfortunately, no conclusion on annual mean PM_{2.5} sensitivities was drawn from these studies.

In Euro_Medi, PM_{2.5} sensitivities are complex and vary from the north to south. The UK and Scandinavia are more sensitive to NH₃ emissions reductions, central Europe is more sensitive to NO_x reductions, while the Mediterranean region is more sensitive to SO_x reductions, which is consistent with conclusions from other European studies (Megaritis et al., 2013; Vieno et al., 2016; Aksoyoglu et al., 2020; Jiang et al., 2020; Clappier et al., 2021). From a perspective of European policy making, it is important to reduce NH₃, NO_x and SO_x emissions together and/or go for stronger reductions to minimise adverse effects caused by enhanced oxidation efficiency. East Asia is another example of mixed sensitivity regimes where individual reductions in SO_x, NO_x and NH₃ emissions are almost equally effective for mitigating PM_{2.5} at a country level. Studies focusing on East Asia highlight the importance of NH₃ emissions control for reducing annual PM_{2.5} pollution especially in central and eastern China (Wang et al., 2011; Pozzer et al., 2017; Cheng et al., 2021). In addition, due to the high proportion of SIA in PM_{2.5} in East Asia, reducing all 3 precursors also produces the greatest reduction in regional average PM_{2.5} compared to other regions. It is possible that the above conclusions may change when considering population-weighted concentration, but we deliberately selected the four most densely populated regions for analysis in order to focus on reductions relevant to human exposure to SIA, so it is anticipated that findings using population weighting would be broadly similar.

Analyses of both 20% and 40% emissions reductions reveal different kinds of linearity and non-linearity. There is considerable non-linearity in the sense of a lack of one-to-one proportionality between an emission reduction and a species concentration or deposition change. Precursor emissions reduction sometimes even increases other pollutant concentrations. This is consequent on interactions in SIA formation, atmospheric oxidizing capacity, and N and S deposition as discussed earlier, and is highly geographically variable. Such non-linearity may be more significant in a certain area during a certain season due to the inter-annual variability in local meteorology and emissions profiles. However, whilst the sensitivity of an annual quantity of a pollutant to emissions reductions is subject to seasonality, we are confident that the broad conclusions of this study will hold, and from a global and regional policymaking perspective, it is more practical to develop policies of reductions in emissions from different sectors and countries on an annual level. Studies focusing on non-proportional responses of European PM_{2.5} to emissions reductions showed that significant seasonality only occurs in a few specific areas (Thunis et al., 2015, 2021; Clappier et al., 2021).

On the other hand, a linearity in response to emissions reductions is apparent via the observation that the responses of PM_{2.5}, N_p, and S_p annual concentrations and deposition components remain essentially proportional to the precursor emissions reductions (20% and 40%) for a given precursor in a given region, albeit that the magnitude of the slope varies substantially with different precursors and regions. Even if the net concentration changes of one species (e.g., PM_{2.5}) induced by reductions in emissions of all 3 precursors are smaller (or greater) than the sum of changes from reductions in individual precursors due to non-linear chemical interactions as discussed earlier, these net changes still follow a very similar gradient when emissions reductions in all 3 precursors change from 20% to 40%. However, where the gradient in the response is not one-to-one, the linearity in the response that is observed up to the 40% emissions reductions simulated here clearly cannot continue to extrapolate linearly all the way to 100% emissions reductions. The gradient of the response must be flatter or steeper (depending on atmospheric component) at the beginning or end of the span from zero to 100% emissions reduction. For instance, 20% and 40% reductions in NH₃ emissions give 24% and 48% decreases in global annual mean NH₃ concentrations respectively (i.e., gradients exceeding one-to-one), whereas these emissions reductions only produce 6% and 14% decreases



in global NH_4^+ concentrations, respectively (i.e., gradients less than one-to-one). When NH_3 emissions are completely switched off, both NH_3 and NH_4^+ concentrations will be zero, so the NH_3 concentration sensitivity must become smaller, and the NH_4^+ concentration sensitivity must become larger as NH_3 emissions reductions approach 100%. Additional serial sensitivity experiments are required to acquire the full spectrum of NH_3 and NH_4^+ (and all other species) sensitivities. It is therefore
735 important for policymakers in different regions to know the emissions reductions required to obtain the mitigation responses needed for specific air quality targets.

Finally, it is also important to remember that reductions in anthropogenic emissions of SIA precursors will have many co-benefits on human health, forests, ecosystem biodiversity, and climate, not just in populated areas but elsewhere.

5 Conclusions

740 The sensitivities of global and regional annual mean surface concentrations and deposition of gaseous and particle N_r and S_r to 20% and 40% reductions in anthropogenic emissions of NH_3 , NO_x , and SO_x both individually and collectively has been investigated using the EMEP MSC-W model coupled with WRF meteorology for 2015. East Asia, South Asia, Euro_Medi, and North America are selected for regional discussions because of their high population densities and N_r and S_r pollution. The comparison in regional responses reveals that the individual emissions reduction in one precursor has multiple co-benefits
745 and sometimes small disbenefits on mitigating N_r , S_r , and $\text{PM}_{2.5}$ pollution, and these effects are highly geographically variable.

From a global policy-making perspective, whilst reductions in NH_3 emissions are effective for decreasing annual NH_3 concentrations and deposition they are considerably less effective at decreasing NH_4^+ . This is because all densely populated continents are ammonia rich so reducing NH_3 emissions only has limited effects on mitigating SIA formation. A 40% reduction in NH_3 emissions decreases regional average NH_3 concentrations in the four regions by 47-49%, while NH_4^+ concentrations
750 decrease in the order Euro_Medi (18%), East Asia (15%), North America (12%), and South Asia (4%), the order of increasing regional ammonia-richness. Other side effects of NH_3 emissions reductions include decreases in annual fine NO_3^- surface concentrations and deposition in the four regions due to reduced NH_4NO_3 formation, and consequently to increased HNO_3 and coarse NO_3^- concentrations and deposition in these regions. Another disbenefit is increased SO_2 surface concentrations in these regions because reduced NH_3 levels affect the pH-dependent SO_2 dry deposition sink. A 40% reduction in NH_3 emissions
755 increases SO_2 concentrations in East Asia by 16%, in South Asia and North America by 14%, and in Euro_Medi by 10%.

Large regional differences are observed in NO_x emissions reduction scenarios. In East Asia, NO_x concentrations are very effectively decreased (by 45%) with 40% NO_x emissions reductions, but they are less effectively decreased in Euro_Medi (38%) and North America (36%) and substantially less effectively decreased in South Asia (22%). By contrast, the regional sensitivities of fine NO_3^- are reversed: South Asia shows the largest decrease (45%), whilst East Asia shows the smallest
760 decrease (33%). This phenomenon is related to different regional oxidation regime and SIA chemistry. NO_x emissions reductions increase O_3 levels in East Asia (and also, but by less, in Euro_Medi), but decrease O_3 levels in South Asia (and also, but by less, in North America). In East Asia, the increased oxidant levels enhance NO_x oxidation efficiency, which results in a larger chemical removal of NO_x . Consequently, the decrease in fine nitrate in East Asia is buffered by its enhanced chemical production. In contrast, decreased oxidant levels in South Asia lessen the oxidation of NO_x and therefore partially
765 offset the decrease in NO_x concentrations due to emissions reductions, and cause a more efficient decrease in fine NO_3^- concentrations. In addition, the reductions in fine NO_3^- levels also cause decreases in NH_4^+ concentrations and deposition and corresponding increases in NH_3 concentrations and deposition, albeit to varying degrees in the different regions. The variations in regional oxidant levels also impact the regional oxidation of SO_2 to SO_4^{2-} . A 40% NO_x emissions reduction causes a 5% decrease in SO_2 and consequently a 3% increase in SO_4^{2-} concentrations in East Asia, but a 2% increase in SO_2 and consequently
770 a 4% decrease in SO_4^{2-} concentrations in South Asia.



775 Reductions in SO_x emissions have globally consistent impacts on SO_2 and SO_4^{2-} concentrations. A 40% reduction in SO_x emissions decreases SO_2 and SO_4^{2-} concentrations in the four regions by 42-45% and 34-38% respectively. Reduced SO_4^{2-} concentrations decrease $(\text{NH}_4)_2\text{SO}_4$ formation but promote NH_4NO_3 formation, which then causes increased NH_3 and fine NO_3^- but decreased NH_4^+ concentrations and deposition. A 40% reduction in SO_x emissions yields ~12% growth in NH_3 total deposition in four regions.

780 $\text{PM}_{2.5}$ sensitivities in South Asia to 40% emissions reductions in precursors individually decrease in the order SO_x (3.10 $\mu\text{g m}^{-3}$, 10%), NO_x (0.97 $\mu\text{g m}^{-3}$, 3%), and NH_3 (0.29 $\mu\text{g m}^{-3}$, 1%), which is consistent with the fact that South Asia is so ammonia-rich that reducing NH_3 hardly has any impacts on mitigating $\text{PM}_{2.5}$. The most effective individual measure for North America is reducing NO_x emissions with an 8% (0.63 $\mu\text{g m}^{-3}$) decrease in regional average $\text{PM}_{2.5}$ in response to a 40% reduction. In Euro_Medi, $\text{PM}_{2.5}$ sensitivities vary from the north to south with regional average sensitivities to 40% reductions in individual precursors in the range 5-8% (0.55-0.82 $\mu\text{g m}^{-3}$). The UK and Scandinavia are more sensitive to NH_3 emissions reductions, central Europe is more sensitive to NO_x emissions reductions, while the Mediterranean is more sensitive to SO_x emissions reductions. East Asia is another example of mixed sensitivity regimes where individual reductions in SO_x , NO_x and NH_3 emissions are almost equally effective for mitigating $\text{PM}_{2.5}$, with regional sensitivities to 40% reductions in the range 7-8% (1.89-2.33 $\mu\text{g m}^{-3}$). Because of the varying contributions of SIA to $\text{PM}_{2.5}$, the relative sensitivities of $\text{PM}_{2.5}$ to 40% reductions in all 3 precursors simultaneously decrease in the order East Asia (5.59 $\mu\text{g m}^{-3}$, 20%), Euro_Medi (1.78 $\mu\text{g m}^{-3}$, 17%), North America (1.31 $\mu\text{g m}^{-3}$, 17%), and South Asia (4.13 $\mu\text{g m}^{-3}$, 13%).

790 The simulations conducted in this work reveals geographically-varying non-linear physicochemical responses of N_r , S_r , and $\text{PM}_{2.5}$ to emissions reductions. It is important not only to prioritise different precursor reductions in different regions, but also reduce emissions of precursors together in order to minimise various disbenefits.

Code and data availability

As described and referenced in Sect. 2 of this paper, this study used two open-source global models: the European Monitoring and Evaluation Programme Meteorological Synthesizing Centre – West atmospheric chemistry transport model (EMEP MSC-W, 2020, version 4.34, source code available at <https://doi.org/10.5281/zenodo.3647990>, last access: 8 Aug 2022) and the Weather Research and Forecasting meteorological model (WRF, version 3.9.1.1, <https://www.wrf-model.org>, last access: 8 Aug 2022; Skamarock et al., 2008). The model outputs presented in figures and tables in this paper and the corresponding Python scripts are available at <https://doi.org/10.5281/zenodo.7082661>, last access: 16 Sep 2022 (Ge, 2022).

Author contribution

800 MH, DS and MV conceptualised and supervised the study. MV and PW contributed to model development and set-up and provided modelling support. MV provided computing resource. YG contributed to study design, undertook all model simulations, formal data analyses, visualisation of the results and data curation, with discussion and refinement by all authors. The original draft of the paper was written by YG with contributions and editing by MH. All authors provided review comments and approval of the final version.

Competing interests

805 The authors declare that they have no conflict of interest.



Acknowledgments

810 Y. Ge gratefully acknowledges studentship funding from the University of Edinburgh and its School of Chemistry. This work was in part supported by the UK Natural Environment Research Council (NERC), including grant nos. NE/R016429/1 and NE/R000131/1, the Department for Environment, Food and Rural Affairs (Defra) contract “Research & Development Support for National Air Pollution Control Strategies (ECM: 62041) 2021 to 2024”, and the European Modelling and Evaluation Programme under the United Nations Economic Commission for Europe Convention on Long-range Transboundary Air Pollution.



815 References

- Aas, W., Mortier, A., Bowersox, V., Cherian, R., Faluvegi, G., Fagerli, H., Hand, J., Klimont, Z., Galy-Lacaux, C., Lehmann, C. M. B., Myhre, C. L., Myhre, G., Olivić, D., Sato, K., Quaas, J., Rao, P. S. P., Schulz, M., Shindell, D., Skeie, R. B., Stein, A., Takemura, T., Tsyro, S., Vet, R., and Xu, X.: Global and regional trends of atmospheric sulfur, *Scientific Reports*, 9, 953, 10.1038/s41598-018-37304-0, 2019.
- 820 Aksoyoglu, S., Jiang, J., Ciarelli, G., Baltensperger, U., and Prévôt, A. S. H.: Role of ammonia in European air quality with changing land and ship emissions between 1990 and 2030, *Atmos. Chem. Phys.*, 20, 15665-15680, 10.5194/acp-20-15665-2020, 2020.
- AQEG: Mitigation of United Kingdom PM_{2.5} Concentrations, Air Quality Expert Group, UK Department for Environment, Food and Rural Affairs, London, PB13837, available
- 825 at: https://uk-air.defra.gov.uk/assets/documents/reports/cat11/1508060903_DEF-PB14161_Mitigation_of_UK_PM25.pdf, 2015.
- Balamurugan, V., Chen, J., Qu, Z., Bi, X., and Keutsch, F. N.: Secondary PM_{2.5} decreases significantly less than NO₂ emission reductions during COVID lockdown in Germany, *Atmos. Chem. Phys.*, 22, 7105-7129, 10.5194/acp-22-7105-2022, 2022.
- 830 Behera, S. N., Sharma, M., Aneja, V. P., and Balasubramanian, R.: Ammonia in the atmosphere: a review on emission sources, atmospheric chemistry and deposition on terrestrial bodies, *Environmental Science and Pollution Research*, 20, 8092-8131, <https://doi.org/10.1007/s11356-013-2051-9>, 2013.
- Berge, E., and Jakobsen, H. A.: A regional scale multilayer model for the calculation of long-term transport and deposition of air pollution in Europe, *Tellus B: Chemical and Physical Meteorology*, 50, 205-223, 10.3402/tellusb.v50i3.16097, 1998.
- 835 Bergström, A.-K., and Jansson, M.: Atmospheric nitrogen deposition has caused nitrogen enrichment and eutrophication of lakes in the northern hemisphere, *Global Change Biology*, 12, 635-643, <https://doi.org/10.1111/j.1365-2486.2006.01129.x>, 2006.
- Bergström, R., Hallquist, M., Simpson, D., Wildt, J., and Mentel, T. F.: Biotic stress: a significant contributor to organic aerosol in Europe?, *Atmos. Chem. Phys.*, 14, 13643-13660, 10.5194/acp-14-13643-2014, 2014.
- 840 Bian, H., Chin, M., Hauglustaine, D. A., Schulz, M., Myhre, G., Bauer, S. E., Lund, M. T., Karydis, V. A., Kucsera, T. L., Pan, X., Pozzer, A., Skeie, R. B., Steenrod, S. D., Sudo, K., Tsigaridis, K., Tsimpidi, A. P., and Tsyro, S. G.: Investigation of global particulate nitrate from the AeroCom phase III experiment, *Atmospheric Chemistry and Physics*, 17, 12911-12940, 10.5194/acp-17-12911-2017, 2017.
- Botha, C. F., Hahn, J., Pienaar, J. J., and Van Eldik, R.: Kinetics and mechanism of the oxidation of sulfur(IV) by ozone in aqueous solutions, *Atmospheric Environment*, 28, 3207-3212, [https://doi.org/10.1016/1352-2310\(94\)00174-J](https://doi.org/10.1016/1352-2310(94)00174-J), 1994.
- 845 Brauer, M., Freedman, G., Frostad, J., van Donkelaar, A., Martin, R. V., Dentener, F., Dingenen, R. v., Estep, K., Amini, H., Apte, J. S., Balakrishnan, K., Barregard, L., Broday, D., Feigin, V., Ghosh, S., Hopke, P. K., Knibbs, L. D., Kokubo, Y., Liu, Y., Ma, S., Morawska, L., Sangrador, J. L. T., Shaddick, G., Anderson, H. R., Vos, T., Forouzanfar, M. H., Burnett, R. T., and Cohen, A.: Ambient Air Pollution Exposure Estimation for the Global Burden of Disease 2013, *Environmental Science & Technology*, 50, 79-88, 10.1021/acs.est.5b03709, 2016.
- 850 Chang, M., Cao, J., Ma, M., Liu, Y., Liu, Y., Chen, W., Fan, Q., Liao, W., Jia, S., and Wang, X.: Dry deposition of reactive nitrogen to different ecosystems across eastern China: A comparison of three community models, *Science of The Total Environment*, 720, 137548, <https://doi.org/10.1016/j.scitotenv.2020.137548>, 2020.
- Chen, C., Zhu, P., Lan, L., Zhou, L., Liu, R., Sun, Q., Ban, J., Wang, W., Xu, D., and Li, T.: Short-term exposures to PM_{2.5} and cause-specific mortality of cardiovascular health in China, *Environmental Research*, 161, 188-194, <https://doi.org/10.1016/j.envres.2017.10.046>, 2018a.
- 855 Chen, L., Shi, M., Gao, S., Li, S., Mao, J., Zhang, H., Sun, Y., Bai, Z., and Wang, Z.: Assessment of population exposure to PM_{2.5} for mortality in China and its public health benefit based on BenMAP, *Environmental Pollution*, 221, 311-317, <https://doi.org/10.1016/j.envpol.2016.11.080>, 2017.
- 860 Chen, X., Wang, Y.-h., Ye, C., Zhou, W., Cai, Z.-c., Yang, H., and Han, X.: Atmospheric Nitrogen Deposition Associated with the Eutrophication of Taihu Lake, *Journal of Chemistry*, 2018, 4017107, 10.1155/2018/4017107, 2018b.
- Cheng, L., Ye, Z., Cheng, S., and Guo, X.: Agricultural ammonia emissions and its impact on PM_{2.5} concentrations in the Beijing-Tianjin-Hebei region from 2000 to 2018, *Environmental Pollution*, 291, 118162, <https://doi.org/10.1016/j.envpol.2021.118162>, 2021.
- 865 Ciarelli, G., Theobald, M. R., Vivanco, M. G., Beekmann, M., Aas, W., Andersson, C., Bergström, R., Manders-Groot, A., Couvidat, F., Mircea, M., Tsyro, S., Fagerli, H., Mar, K., Raffort, V., Roustan, Y., Pay, M. T., Schaap, M., Kranenburg, R., Adani, M., Briganti, G., Cappelletti, A., D'Isidoro, M., Cuvelier, C., Cholakian, A., Bessagnet, B., Wind, P., and Colette, A.: Trends of inorganic and organic aerosols and precursor gases in Europe: insights from the EURODELTA multi-model experiment over the 1990–2010 period, *Geoscientific Model Development*, 12, 4923-4954, 10.5194/gmd-12-4923-2019, 2019.
- 870 Clappier, A., Thunis, P., Beekmann, M., Putaud, J. P., and de Meij, A.: Impact of SO_x, NO_x and NH₃ emission reductions on PM_{2.5} concentrations across Europe: Hints for future measure development, *Environment International*, 156, 106699, <https://doi.org/10.1016/j.envint.2021.106699>, 2021.
- Crippa, M., Solazzo, E., Huang, G., Guizzardi, D., Koffi, E., Muntean, M., Schieberle, C., Friedrich, R., and Janssens-Maenhout, G.: High resolution temporal profiles in the Emissions Database for Global Atmospheric Research, *Scientific Data*, 7, 121, 10.1038/s41597-020-0462-2, 2020.
- 875



- EEA: Air quality in Europe – 2021 report. EEA Report No. 15/2021., European Environment Agency, Publications Office of the European Union, available at: <https://www.eea.europa.eu/publications/air-quality-in-europe-2021/> (last access: 7 August 2022), 2021.
- 880 Erisman, J. W., Hensen, A., Fowler, D., Flechard, C. R., Grüner, A., Spindler, G., Duyzer, J. H., Weststrate, H., Römer, F., Vonk, A. W., and Jaarsveld, H. v.: Dry Deposition Monitoring in Europe, *Water, Air and Soil Pollution: Focus*, 1, 17-27, 10.1023/A:1013105727252, 2001.
- Erisman, J. W., Domburg, N., de Vries, W., Kros, H., de Haan, B., and Sanders, K.: The Dutch N-cascade in the European perspective, *Science in China Series C: Life Sciences*, 48, 827-842, <https://doi.org/10.1007/BF03187122>, 2005.
- 885 Fang, Y., Ye, C., Wang, J., Wu, Y., Hu, M., Lin, W., Xu, F., and Zhu, T.: Relative humidity and O₃ concentration as two prerequisites for sulfate formation, *Atmos. Chem. Phys.*, 19, 12295-12307, 10.5194/acp-19-12295-2019, 2019.
- Fowler, D., Pilegaard, K., Sutton, M. A., Ambus, P., Raivonen, M., Duyzer, J., Simpson, D., Fagerli, H., Fuzzi, S., Schjoerring, J. K., Granier, C., Neff, A., Isaksen, I. S. A., Laj, P., Maione, M., Monks, P. S., Burkhardt, J., Daemmgen, U., Neirynek, J., Personne, E., Wichink-Kruit, R., Butterbach-Bahl, K., Flechard, C., Tuovinen, J. P., Coyle, M., Gerosa, G., Loubet, B., Altimir, N., Gruenhage, L., Ammann, C., Cieslik, S., Paoletti, E., Mikkelsen, T. N., Ro-Poulsen, H., Cellier, P., Cape, J. N., Horváth, L., Loreto, F., Niinemets, Ü., Palmer, P. I., Rinne, J., Misztal, P., Nemitz, E., Nilsson, D., Pryor, S., Gallagher, M. W., Vesala, T., Skiba, U., Brüggemann, N., Zechmeister-Boltenstern, S., Williams, J., O'Dowd, C., Facchini, M. C., de Leeuw, G., Flossman, A., Chaumerliac, N., and Erisman, J. W.: Atmospheric composition change: Ecosystems–Atmosphere interactions, *Atmospheric Environment*, 43, 5193-5267, <https://doi.org/10.1016/j.atmosenv.2009.07.068>, 2009.
- 890 Fowler, D., Steadman, C. E., Stevenson, D., Coyle, M., Rees, R. M., Skiba, U. M., Sutton, M. A., Cape, J. N., Dore, A. J., Vieno, M., Simpson, D., Zechle, S., Stocker, B. D., Rinaldi, M., Facchini, M. C., Flechard, C. R., Nemitz, E., Twigg, M., Erisman, J. W., Butterbach-Bahl, K., and Galloway, J. N.: Effects of global change during the 21st century on the nitrogen cycle, *Atmospheric Chemistry and Physics*, 15, 13849-13893, 10.5194/acp-15-13849-2015, 2015.
- Fowler, D., Brimblecombe, P., Burrows, J., Heal, M. R., Grennfelt, P., Stevenson, D. S., Jowett, A., Nemitz, E., Coyle, M., Liu, X., Chang, Y., Fuller, G. W., Sutton, M. A., Klimont, Z., Unsworth, M. H., and Vieno, M.: A chronology of global air quality, *Philosophical Transactions of the Royal Society A: Mathematical, Physical and Engineering Sciences*, 378, 20190314, 10.1098/rsta.2019.0314, 2020.
- 900 Fu, X., Wang, T., Gao, J., Wang, P., Liu, Y., Wang, S., Zhao, B., and Xue, L.: Persistent Heavy Winter Nitrate Pollution Driven by Increased Photochemical Oxidants in Northern China, *Environmental Science & Technology*, 54, 3881-3889, 10.1021/acs.est.9b07248, 2020.
- 905 Ge, W., Liu, J., Yi, K., Xu, J., Zhang, Y., Hu, X., Ma, J., Wang, X., Wan, Y., Hu, J., Zhang, Z., Wang, X., and Tao, S.: Influence of atmospheric in-cloud aqueous-phase chemistry on the global simulation of SO₂ in CESM2, *Atmos. Chem. Phys.*, 21, 16093-16120, 10.5194/acp-21-16093-2021, 2021a.
- Ge, Y., Heal, M. R., Stevenson, D. S., Wind, P., and Vieno, M.: Evaluation of global EMEP MSC-W (rv4.34) WRF (v3.9.1.1) model surface concentrations and wet deposition of reactive N and S with measurements, *Geosci. Model Dev.*, 14, 7021-7046, 10.5194/gmd-14-7021-2021, 2021b.
- 910 Ge, Y.: Dataset for global sensitivities of reactive N and S gas and particle concentrations and deposition to precursor emissions reductions [Data set], Zenodo, 10.5281/zenodo.7082661, 2022.
- Ge, Y., Vieno, M., Stevenson, D. S., Wind, P., and Heal, M. R.: A new assessment of global and regional budgets, fluxes, and lifetimes of atmospheric reactive N and S gases and aerosols, *Atmos. Chem. Phys.*, 22, 8343-8368, 10.5194/acp-22-8343-2022, 2022.
- 915 Gu, B., Zhang, L., Van Dingenen, R., Vieno, M., Van Grinsven, H. J. M., Zhang, X., Zhang, S., Chen, Y., Wang, S., Ren, C., Rao, S., Holland, M., Winiwarter, W., Chen, D., Xu, J., and Sutton, M. A.: Abating ammonia is more cost-effective than nitrogen oxides for mitigating PM_{2.5} air pollution, *Science*, 374, 758-762, 10.1126/science.abf8623, 2021.
- Hart, J. E., Liao, X., Hong, B., Puett, R. C., Yanosky, J. D., Suh, H., Kioumourtzoglou, M.-A., Spiegelman, D., and Laden, F.: The association of long-term exposure to PM_{2.5} on all-cause mortality in the Nurses' Health Study and the impact of measurement-error correction, *Environmental Health*, 14, 38, 10.1186/s12940-015-0027-6, 2015.
- Hattori, S., Iizuka, Y., Alexander, B., Ishino, S., Fujita, K., Zhai, S., Sherwen, T., Oshima, N., Uemura, R., Yamada, A., Suzuki, N., Matoba, S., Tsuruta, A., Savarino, J., and Yoshida, N.: Isotopic evidence for acidity-driven enhancement of sulfate formation after SO₂ emission control, *Science Advances*, 7, eabd4610, 10.1126/sciadv.abd4610, 2021.
- 925 Hauglustaine, D. A., Balkanski, Y., and Schulz, M.: A global model simulation of present and future nitrate aerosols and their direct radiative forcing of climate, *Atmospheric Chemistry and Physics*, 14, 11031-11063, 10.5194/acp-14-11031-2014, 2014.
- Heald, C. L., Collett Jr, J. L., Lee, T., Benedict, K. B., Schwandner, F. M., Li, Y., Clarisse, L., Hurtmans, D. R., Van Damme, M., Clerbaux, C., Coheur, P. F., Philip, S., Martin, R. V., and Pye, H. O. T.: Atmospheric ammonia and particulate inorganic nitrogen over the United States, *Atmos. Chem. Phys.*, 12, 10295-10312, 10.5194/acp-12-10295-2012, 2012.
- 930 Hoesly, R. M., Smith, S. J., Feng, L., Klimont, Z., Janssens-Maenhout, G., Pitkanen, T., Seibert, J. J., Vu, L., Andres, R. J., Bolt, R. M., Bond, T. C., Dawidowski, L., Kholod, N., Kurokawa, J. I., Li, M., Liu, L., Lu, Z., Moura, M. C. P., O'Rourke, P. R., and Zhang, Q.: Historical (1750–2014) anthropogenic emissions of reactive gases and aerosols from the Community Emissions Data System (CEDS), *Geosci. Model Dev.*, 11, 369-408, 10.5194/gmd-11-369-2018, 2018.
- Hoffmann, E. H., Tilgner, A., Schrödner, R., Bräuer, P., Wolke, R., and Herrmann, H.: An advanced modeling study on the impacts and atmospheric implications of multiphase dimethyl sulfide chemistry, *Proceedings of the National Academy of Sciences*, 113, 11776, 10.1073/pnas.1606320113, 2016.
- 935 Hoffmann, M. R.: On the kinetics and mechanism of oxidation of aequated sulfur dioxide by ozone, *Atmospheric Environment* (1967), 20, 1145-1154, [https://doi.org/10.1016/0004-6981\(86\)90147-2](https://doi.org/10.1016/0004-6981(86)90147-2), 1986.



- Holt, J., Selin, N. E., and Solomon, S.: Changes in Inorganic Fine Particulate Matter Sensitivities to Precursors Due to Large-Scale US Emissions Reductions, *Environmental Science & Technology*, 49, 4834-4841, 10.1021/acs.est.5b00008, 2015.
- 940 Iturbide, M., Gutiérrez, J. M., Alves, L. M., Bedia, J., Cerezo-Mota, R., Cimadevilla, E., Cofiño, A. S., Di Luca, A., Faria, S. H., Gorodetskaya, I. V., Hauser, M., Herrera, S., Hennessy, K., Hewitt, H. T., Jones, R. G., Krakovska, S., Manzanar, R., Martínez-Castro, D., Narisma, G. T., Nurhati, I. S., Pinto, L., Seneviratne, S. I., van den Hurk, B., and Vera, C. S.: An update of IPCC climate reference regions for subcontinental analysis of climate model data: definition and aggregated datasets, *Earth Syst. Sci. Data*, 12, 2959-2970, 10.5194/essd-12-2959-2020, 2020.
- 945 Jiang, J., Aksoyoglu, S., Ciarelli, G., Baltensperger, U., and Prévôt, A. S. H.: Changes in ozone and PM_{2.5} in Europe during the period of 1990–2030: Role of reductions in land and ship emissions, *Science of The Total Environment*, 741, 140467, <https://doi.org/10.1016/j.scitotenv.2020.140467>, 2020.
- 950 Jonson, J. E., Borken-Kleefeld, J., Simpson, D., Nyíri, A., Posch, M., and Heyes, C.: Impact of excess NO_x emissions from diesel cars on air quality, public health and eutrophication in Europe, *Environmental Research Letters*, 12, 094017, 10.1088/1748-9326/aa8850, 2017.
- Jonson, J. E., Fagerli, H., Scheuschner, T., and Tsyro, S.: Modelling changes in secondary inorganic aerosol formation and nitrogen deposition in Europe from 2005 to 2030, *Atmos. Chem. Phys.*, 22, 1311-1331, 10.5194/acp-22-1311-2022, 2022.
- 955 Jovan, S., Riddell, J., Padgett, P. E., and Nash Iii, T. H.: Eutrophic lichens respond to multiple forms of N: implications for critical levels and critical loads research, *Ecological Applications*, 22, 1910-1922, <https://doi.org/10.1890/11-2075.1>, 2012.
- Karimi, A., Shirmardi, M., Hadei, M., Birgani, Y. T., Neisi, A., Takdastan, A., and Goudarzi, G.: Concentrations and health effects of short- and long-term exposure to PM_{2.5}, NO₂, and O₃ in ambient air of Ahvaz city, Iran (2014–2017), *Ecotoxicology and Environmental Safety*, 180, 542-548, <https://doi.org/10.1016/j.ecoenv.2019.05.026>, 2019.
- 960 Karl, M., Jonson, J. E., Uppstu, A., Aulinger, A., Prank, M., Sofiev, M., Jalkanen, J. P., Johansson, L., Quante, M., and Matthias, V.: Effects of ship emissions on air quality in the Baltic Sea region simulated with three different chemistry transport models, *Atmos. Chem. Phys.*, 19, 7019-7053, 10.5194/acp-19-7019-2019, 2019.
- Kelly, J. T., Jang, C., Zhu, Y., Long, S., Xing, J., Wang, S., Murphy, B. N., and Pye, H. O. T.: Predicting the Nonlinear Response of PM_{2.5} and Ozone to Precursor Emission Changes with a Response Surface Model, *Atmosphere*, 12, 10.3390/atmos12081044, 2021.
- 965 Kharol, S. K., Shephard, M. W., McLinden, C. A., Zhang, L., Sioris, C. E., O'Brien, J. M., Vet, R., Cady-Pereira, K. E., Hare, E., Siemons, J., and Krotkov, N. A.: Dry Deposition of Reactive Nitrogen From Satellite Observations of Ammonia and Nitrogen Dioxide Over North America, *Geophysical Research Letters*, 45, 1157-1166, <https://doi.org/10.1002/2017GL075832>, 2018.
- Kurokawa, J., and Ohara, T.: Long-term historical trends in air pollutant emissions in Asia: Regional Emission inventory in ASia (REAS) version 3, *Atmos. Chem. Phys.*, 20, 12761-12793, 10.5194/acp-20-12761-2020, 2020.
- 970 Le, T., Wang, Y., Liu, L., Yang, J., Yung, Y. L., Li, G., and Seinfeld, J. H.: Unexpected air pollution with marked emission reductions during the COVID-19 outbreak in China, *Science*, 369, 702-706, 10.1126/science.abb7431, 2020.
- Leung, D. M., Shi, H., Zhao, B., Wang, J., Ding, E. M., Gu, Y., Zheng, H., Chen, G., Liou, K.-N., Wang, S., Fast, J. D., Zheng, G., Jiang, J., Li, X., and Jiang, J. H.: Wintertime Particulate Matter Decrease Buffered by Unfavorable Chemical Processes Despite Emissions Reductions in China, *Geophysical Research Letters*, 47, e2020GL087721, <https://doi.org/10.1029/2020GL087721>, 2020.
- 975 Li, L., Chen, Z. M., Zhang, Y. H., Zhu, T., Li, J. L., and Ding, J.: Kinetics and mechanism of heterogeneous oxidation of sulfur dioxide by ozone on surface of calcium carbonate, *Atmos. Chem. Phys.*, 6, 2453-2464, 10.5194/acp-6-2453-2006, 2006.
- 980 Liang, J., and Jacobson, M. Z.: A study of sulfur dioxide oxidation pathways over a range of liquid water contents, pH values, and temperatures, *Journal of Geophysical Research: Atmospheres*, 104, 13749-13769, <https://doi.org/10.1029/1999JD900097>, 1999.
- Liao, K.-J., Tagaris, E., Napelenok, S. L., Manomaiphiboon, K., Woo, J.-H., Amar, P., He, S., and Russell, A. G.: Current and Future Linked Responses of Ozone and PM_{2.5} to Emission Controls, *Environmental Science & Technology*, 42, 4670-4675, 10.1021/es7028685, 2008.
- 985 Liu, F., Zhang, Q., van der A, R. J., Zheng, B., Tong, D., Yan, L., Zheng, Y., and He, K.: Recent reduction in NO_x emissions over China: synthesis of satellite observations and emission inventories, *Environmental Research Letters*, 11, 114002, 10.1088/1748-9326/11/11/114002, 2016.
- Liu, M., Huang, X., Song, Y., Xu, T., Wang, S., Wu, Z., Hu, M., Zhang, L., Zhang, Q., Pan, Y., Liu, X., and Zhu, T.: Rapid SO₂ emission reductions significantly increase tropospheric ammonia concentrations over the North China Plain, *Atmos. Chem. Phys.*, 18, 17933-17943, 10.5194/acp-18-17933-2018, 2018.
- 990 Lu, Z., Streets, D. G., Zhang, Q., Wang, S., Carmichael, G. R., Cheng, Y. F., Wei, C., Chin, M., Diehl, T., and Tan, Q.: Sulfur dioxide emissions in China and sulfur trends in East Asia since 2000, *Atmos. Chem. Phys.*, 10, 6311-6331, 10.5194/acp-10-6311-2010, 2010.
- 995 Ma, Z., Hu, X., Huang, L., Bi, J., and Liu, Y.: Estimating Ground-Level PM_{2.5} in China Using Satellite Remote Sensing, *Environmental Science & Technology*, 48, 7436-7444, 10.1021/es5009399, 2014.
- Maahs, H. G.: Kinetics and mechanism of the oxidation of S(IV) by ozone in aqueous solution with particular reference to SO₂ conversion in nonurban tropospheric clouds, *Journal of Geophysical Research: Oceans*, 88, 10721-10732, <https://doi.org/10.1029/JC088iC15p10721>, 1983.
- 1000 Massad, R. S., Nemitz, E., and Sutton, M. A.: Review and parameterisation of bi-directional ammonia exchange between vegetation and the atmosphere, *Atmos. Chem. Phys.*, 10, 10359-10386, 10.5194/acp-10-10359-2010, 2010.
- McArdle, J. V., and Hoffmann, M. R.: Kinetics and mechanism of the oxidation of aquated sulfur dioxide by hydrogen peroxide at low pH, *The Journal of Physical Chemistry*, 87, 5425-5429, 10.1021/j150644a024, 1983.



- 1005 McFiggans, G., Mentel, T. F., Wildt, J., Pullinen, I., Kang, S., Kleist, E., Schmitt, S., Springer, M., Tillmann, R., Wu, C., Zhao, D., Hallquist, M., Faxon, C., Le Breton, M., Hallquist, Å. M., Simpson, D., Bergström, R., Jenkin, M. E., Ehn, M., Thornton, J. A., Alfarra, M. R., Bannan, T. J., Percival, C. J., Priestley, M., Topping, D., and Kiendler-Scharr, A.: Secondary organic aerosol reduced by mixture of atmospheric vapours, *Nature*, 565, 587–593, 10.1038/s41586-018-0871-y, 2019.
- 1010 McHale, M. R., Ludtke, A. S., Wetherbee, G. A., Burns, D. A., Nilles, M. A., and Finkelstein, J. S.: Trends in precipitation chemistry across the U.S. 1985–2017: Quantifying the benefits from 30 years of Clean Air Act amendment regulation, *Atmospheric Environment*, 247, 118219, <https://doi.org/10.1016/j.atmosenv.2021.118219>, 2021.
- 1015 Megaritis, A. G., Fountoukis, C., Charalampidis, P. E., Pilinis, C., and Pandis, S. N.: Response of fine particulate matter concentrations to changes of emissions and temperature in Europe, *Atmos. Chem. Phys.*, 13, 3423–3443, 10.5194/acp-13-3423-2013, 2013.
- 1020 Meng, F., Zhang, Y., Kang, J., Heal, M. R., Reis, S., Wang, M., Liu, L., Wang, K., Yu, S., Li, P., Wei, J., Hou, Y., Zhang, Y., Liu, X., Cui, Z., Xu, W., and Zhang, F.: Trends in secondary inorganic aerosol pollution in China and its responses to emission controls of precursors in wintertime, *Atmos. Chem. Phys.*, 22, 6291–6308, 10.5194/acp-22-6291-2022, 2022.
- 1025 Metzger, S., Steil, B., Abdelkader, M., Klingmüller, K., Xu, L., Penner, J. E., Fountoukis, C., Nenes, A., and Lelieveld, J.: Aerosol water parameterisation: a single parameter framework, *Atmos. Chem. Phys.*, 16, 7213–7237, 10.5194/acp-16-7213-2016, 2016.
- 1030 Metzger, S., Abdelkader, M., Steil, B., and Klingmüller, K.: Aerosol water parameterization: long-term evaluation and importance for climate studies, *Atmos. Chem. Phys.*, 18, 16747–16774, 10.5194/acp-18-16747-2018, 2018.
- 1035 NEC: National Emission Ceilings (NEC) Directive reporting status, Briefing no. 2/2019, PDF TH-AM-19-003-EN-N, available at: <https://www.eea.europa.eu/themes/air/air-pollution-sources-1/national-emission-ceilings/nec-directive-reporting-status-2019> (last access: 07 August 2022), 2019.
- 1040 Nenes, A., Pandis, S. N., Weber, R. J., and Russell, A.: Aerosol pH and liquid water content determine when particulate matter is sensitive to ammonia and nitrate availability, *Atmos. Chem. Phys.*, 20, 3249–3258, 10.5194/acp-20-3249-2020, 2020.
- 1045 Novak, G. A., Kilgour, D. B., Jernigan, C. M., Vermeuel, M. P., and Bertram, T. H.: Oceanic emissions of dimethyl sulfide and methanethiol and their contribution to sulfur dioxide production in the marine atmosphere, *Atmos. Chem. Phys.*, 22, 6309–6325, 10.5194/acp-22-6309-2022, 2022.
- 1050 Penkett, S. A., Jones, B. M. R., Brich, K. A., and Eggleton, A. E. J.: The importance of atmospheric ozone and hydrogen peroxide in oxidising sulphur dioxide in cloud and rainwater, *Atmospheric Environment* (1967), 13, 123–137, [https://doi.org/10.1016/0004-6981\(79\)90251-8](https://doi.org/10.1016/0004-6981(79)90251-8), 1979.
- 1055 Pescott, O. L., Simkin, J. M., August, T. A., Randle, Z., Dore, A. J., and Botham, M. S.: Air pollution and its effects on lichens, bryophytes, and lichen-feeding Lepidoptera: review and evidence from biological records, *Biological Journal of the Linnean Society*, 115, 611–635, 10.1111/bij.12541, 2015.
- 1060 Pommier, M., Fagerli, H., Gauss, M., Simpson, D., Sharma, S., Sinha, V., Ghude, S. D., Landgren, O., Nyiri, A., and Wind, P.: Impact of regional climate change and future emission scenarios on surface O₃ and PM_{2.5} over India, *Atmos. Chem. Phys.*, 18, 103–127, 10.5194/acp-18-103-2018, 2018.
- 1065 Pommier, M., Fagerli, H., Schulz, M., Valdebenito, A., Kranenburg, R., and Schaap, M.: Prediction of source contributions to urban background PM₁₀ concentrations in European cities: a case study for an episode in December 2016 using EMEP/MS-CW rv4.15 and LOTOS-EUROS v2.0 – Part 1: The country contributions, *Geoscientific Model Development*, 13, 1787–1807, 10.5194/gmd-13-1787-2020, 2020.
- 1070 Pozzer, A., Tsimpidi, A. P., Karydis, V. A., de Meij, A., and Lelieveld, J.: Impact of agricultural emission reductions on fine-particulate matter and public health, *Atmos. Chem. Phys.*, 17, 12813–12826, 10.5194/acp-17-12813-2017, 2017.
- 1075 Quinn, P. K., and Bates, T. S.: The case against climate regulation via oceanic phytoplankton sulphur emissions, *Nature*, 480, 51–56, 10.1038/nature10580, 2011.
- 1080 Saylor, R., Myles, L., Sibble, D., Caldwell, J., and Xing, J.: Recent trends in gas-phase ammonia and PM_{2.5} ammonium in the Southeast United States, *Journal of the Air & Waste Management Association*, 65, 347–357, 10.1080/10962247.2014.992554, 2015.
- 1085 Seinfeld, J. H., and Pandis, S. N.: *Atmospheric chemistry and physics: from air pollution to climate change*, John Wiley & Sons, 2016.
- 1090 Sheng, F., Jingjing, L., Yu, C., Fu-Ming, T., Xuemei, D., and Jing-yao, L.: Theoretical study of the oxidation reactions of sulfurous acid/sulfite with ozone to produce sulfuric acid/sulfate with atmospheric implications, *RSC Advances*, 8, 7988–7996, 10.1039/C8RA00411K, 2018.
- 1095 Sheppard, L. J., Leith, I. D., Mizunuma, T., Neil Cape, J., Crossley, A., Leeson, S., Sutton, M. A., van Dijk, N., and Fowler, D.: Dry deposition of ammonia gas drives species change faster than wet deposition of ammonium ions: evidence from a long-term field manipulation, *Global Change Biology*, 17, 3589–3607, <https://doi.org/10.1111/j.1365-2486.2011.02478.x>, 2011.
- 1100 Simpson, D., Benedictow, A., Berge, H., Bergström, R., Emberson, L. D., Fagerli, H., Flechard, C. R., Hayman, G. D., Gauss, M., Jonson, J. E., Jenkin, M. E., Nyíri, A., Richter, C., Semeena, V. S., Tsyro, S., Tuovinen, J. P., Valdebenito, A., and Wind, P.: The EMEP MSC-W chemical transport model — technical description, *Atmos. Chem. Phys.*, 12, 7825–7865, 10.5194/acp-12-7825-2012, 2012.
- 1105 Simpson, D., Schulz, M., Semeena, V. S., Tsyro, S., Valdebenito, A., Wind, P., and Steensen, B. M.: EMEP model development and performance changes, in *EMEP Status Report 1/2013*, Norwegian Meteorological Institute, Oslo, Norway, www.emep.int, 45–57, https://emep.int/publ/reports/2013/EMEP_status_report_1_2013.pdf, 2013.
- 1110 Simpson, D., Tsyro, S., and Wind, P.: Updates to the EMEP/MS-CW model, in *EMEP Status Report 1/2015*, Norwegian Meteorological Institute, Oslo, Norway, www.emep.int, 129–136, https://emep.int/publ/reports/2015/EMEP_Status_Report_1_2015.pdf, 2015.



- Simpson, D., Nyíri, A. g., Tsyro, S., Valdebenito, Á., and Wind, P.: Updates to the EMEP/MSC-W model, 2015-2016, in EMEP Status Report 1/2016, Norwegian Meteorological Institute, Oslo, Norway, [www.emep.int](https://emep.int/publ/reports/2016/EMEP_Status_Report_1_2016.pdf), 131-138, https://emep.int/publ/reports/2016/EMEP_Status_Report_1_2016.pdf, 2016.
- 1070 Simpson, D., Bergström, R., Imhof, H., and Wind, P.: Updates to the EMEP/MSC-W model 2016--2017, in EMEP Status Report 1/2017, Norwegian Meteorological Institute, Oslo, Norway, [www.emep.int](https://emep.int/publ/reports/2017/EMEP_Status_Report_1_2017.pdf), 115-122, https://emep.int/publ/reports/2017/EMEP_Status_Report_1_2017.pdf, 2017.
- Simpson, D., Wind, P., Bergström, R., Gauss, M., Tsyro, S., and Valdebenito, Á.: Updates to the EMEP MSC-W model 2017-2018, in EMEP Status Report 1/2018, Norwegian Meteorological Institute, Oslo, Norway, [www.emep.int](https://emep.int/publ/reports/2018/EMEP_Status_Report_1_2018.pdf), 107-115, https://emep.int/publ/reports/2018/EMEP_Status_Report_1_2018.pdf, 2018.
- 1075 Simpson, D., Bergström, R., Tsyro, S., and Wind, P.: Updates to the EMEP/MSC-W model 2018--2019, in EMEP Status Report 1/2019, Norwegian Meteorological Institute, Oslo, Norway, [www.emep.int](https://emep.int/publ/reports/2019/EMEP_Status_Report_1_2019.pdf), 143-152, https://emep.int/publ/reports/2019/EMEP_Status_Report_1_2019.pdf, 2019.
- Simpson, D., Bergström, R., Tsyro, S., and Wind, P.: Updates to the EMEP MSC-W model 2019--2020, in EMEP Status Report 1/2020, Norwegian Meteorological Institute, Oslo, Norway, [www.emep.int](https://emep.int/publ/reports/2020/EMEP_Status_Report_1_2020.pdf), 153-163, https://emep.int/publ/reports/2020/EMEP_Status_Report_1_2020.pdf, 2020.
- 1080 Skamarock, W. C., Klemp, J. B., Dudhia, J., Gill, D. O., Barker, D., Duda, M. G., Huang, X. Y., Wang, W., and Powers, J. G.: A Description of the Advanced Research WRF Version 3 (No. NCAR/TN-475+STR), University Corporation for Atmospheric Research, 113, 10.5065/D68S4MVH, 2008.
- 1085 Smith, R. I., Fowler, D., Sutton, M. A., Flechard, C., and Coyle, M.: Regional estimation of pollutant gas dry deposition in the UK: model description, sensitivity analyses and outputs, *Atmospheric Environment*, 34, 3757-3777, [https://doi.org/10.1016/S1352-2310\(99\)00517-8](https://doi.org/10.1016/S1352-2310(99)00517-8), 2000.
- Stieb, D. M., Evans, G. J., To, T. M., Brook, J. R., and Burnett, R. T.: An ecological analysis of long-term exposure to PM_{2.5} and incidence of COVID-19 in Canadian health regions, *Environmental Research*, 191, 110052, <https://doi.org/10.1016/j.envres.2020.110052>, 2020.
- 1090 Sun, J., Fu, J. S., Lynch, J. A., Huang, K., and Gao, Y.: Climate-driven exceedance of total (wet + dry) nitrogen (N) + sulfur (S) deposition to forest soil over the conterminous U.S., *Earth's Future*, 5, 560-576, <https://doi.org/10.1002/2017EF000588>, 2017.
- Sutton, M. A., Mason, K. E., Sheppard, L. J., Sverdrup, H., Haeuber, R., and Hicks, W. K.: Nitrogen Deposition, *Critical Loads and Biodiversity*, Springer, Dordrecht, 535 pp., 2014.
- 1095 Sutton, M. A., van Dijk, N., Levy, P. E., Jones, M. R., Leith, I. D., Sheppard, L. J., Leeson, S., Sim Tang, Y., Stephens, A., Braban, C. F., Dragosits, U., Howard, C. M., Vieno, M., Fowler, D., Corbett, P., Naikoo, M. I., Munzi, S., Ellis, C. J., Chatterjee, S., Steadman, C. E., Möring, A., and Wolsley, P. A.: Alkaline air: changing perspectives on nitrogen and air pollution in an ammonia-rich world, *Philosophical Transactions of the Royal Society A: Mathematical, Physical and Engineering Sciences*, 378, 20190315, [10.1098/rsta.2019.0315](https://doi.org/10.1098/rsta.2019.0315), 2020.
- 1100 Theobald, M. R., Vivanco, M. G., Aas, W., Andersson, C., Ciarelli, G., Couvidat, F., Cuvelier, K., Manders, A., Mircea, M., Pay, M. T., Tsyro, S., Adani, M., Bergström, R., Bessagnet, B., Briganti, G., Cappelletti, A., D'Isidoro, M., Fagerli, H., Mar, K., Otero, N., Raffort, V., Roustan, Y., Schaap, M., Wind, P., and Colette, A.: An evaluation of European nitrogen and sulfur wet deposition and their trends estimated by six chemistry transport models for the period 1990--2010, *Atmos. Chem. Phys.*, 19, 379-405, [10.5194/acp-19-379-2019](https://doi.org/10.5194/acp-19-379-2019), 2019.
- 1105 Thunis, P., Clappier, A., Pisoni, E., and Degraeuwe, B.: Quantification of non-linearities as a function of time averaging in regional air quality modeling applications, *Atmospheric Environment*, 103, 263-275, <https://doi.org/10.1016/j.atmosenv.2014.12.057>, 2015.
- 1110 Thunis, P., Clappier, A., Beekmann, M., Putaud, J. P., Cuvelier, C., Madrazo, J., and de Meij, A.: Non-linear response of PM_{2.5} to changes in NO_x and NH₃ emissions in the Po basin (Italy): consequences for air quality plans, *Atmos. Chem. Phys.*, 21, 9309-9327, [10.5194/acp-21-9309-2021](https://doi.org/10.5194/acp-21-9309-2021), 2021.
- Tørseth, K., Aas, W., Breivik, K., Fjæraa, A. M., Fiebig, M., Hjellbrekke, A. G., Lund Myhre, C., Solberg, S., and Yttri, K. E.: Introduction to the European Monitoring and Evaluation Programme (EMEP) and observed atmospheric composition change during 1972-2009, *Atmos. Chem. Phys.*, 12, 5447-5481, [10.5194/acp-12-5447-2012](https://doi.org/10.5194/acp-12-5447-2012), 2012.
- 1115 Tsimpidi, A. P., Karydis, V. A., and Pandis, S. N.: Response of Inorganic Fine Particulate Matter to Emission Changes of Sulfur Dioxide and Ammonia: The Eastern United States as a Case Study, *Journal of the Air & Waste Management Association*, 57, 1489-1498, [10.3155/1047-3289.57.12.1489](https://doi.org/10.3155/1047-3289.57.12.1489), 2007.
- Tsimpidi, A. P., Karydis, V. A., and Pandis, S. N.: Response of Fine Particulate Matter to Emission Changes of Oxides of Nitrogen and Anthropogenic Volatile Organic Compounds in the Eastern United States, *Journal of the Air & Waste Management Association*, 58, 1463-1473, [10.3155/1047-3289.58.11.1463](https://doi.org/10.3155/1047-3289.58.11.1463), 2008.
- 1120 Tsyro, S., Karl, M., Simpson, D., Valdebenito, A. I., and Wind, P.: Updates to the EMEP/MSC-W model, in EMEP Status Report 1/2014, Norwegian Meteorological Institute, Oslo, Norway, [www.emep.int](https://emep.int/publ/reports/2014/EMEP_Status_Report_1_2014.pdf), 143-146, https://emep.int/publ/reports/2014/EMEP_Status_Report_1_2014.pdf, 2014.
- USEPA: Report on the Environment: Particulate Matter Concentrations., United States Environmental Protection Agency, available at : <https://cfpub.epa.gov/roe/indicator.cfm?i=9> (last access: 7 August 2022), 2017.
- 1125 Van Herk, C. M., Mathijssen-Spiekman, E. A. M., and de Zwart, D.: Long distance nitrogen air pollution effects on lichens in Europe, *The Lichenologist*, 35, 347-359, [10.1016/S0024-2829\(03\)00036-7](https://doi.org/10.1016/S0024-2829(03)00036-7), 2003.
- Vasilakos, P., Russell, A., Weber, R., and Nenes, A.: Understanding nitrate formation in a world with less sulfate, *Atmos. Chem. Phys.*, 18, 12765-12775, [10.5194/acp-18-12765-2018](https://doi.org/10.5194/acp-18-12765-2018), 2018.



- 1130 Vieno, M., Dore, A. J., Stevenson, D. S., Doherty, R., Heal, M. R., Reis, S., Hallsworth, S., Tarrason, L., Wind, P., Fowler, D., Simpson, D., and Sutton, M. A.: Modelling surface ozone during the 2003 heat-wave in the UK, *Atmospheric Chemistry and Physics*, 10, 7963-7978, 10.5194/acp-10-7963-2010, 2010.
Vieno, M., Heal, M. R., Hallsworth, S., Famulari, D., Doherty, R. M., Dore, A. J., Tang, Y. S., Braban, C. F., Leaver, D., Sutton, M. A., and Reis, S.: The role of long-range transport and domestic emissions in determining atmospheric secondary inorganic particle concentrations across the UK, *Atmos. Chem. Phys.*, 14, 8435-8447, 10.5194/acp-14-8435-2014, 2014.
- 1135 Vieno, M., Heal, M. R., Williams, M. L., Carnell, E. J., Nemitz, E., Stedman, J. R., and Reis, S.: The sensitivities of emissions reductions for the mitigation of UK PM_{2.5}, *Atmospheric Chemistry and Physics*, 16, 265-276, 10.5194/acp-16-265-2016, 2016.
- 1140 Wang, S., Xing, J., Jang, C., Zhu, Y., Fu, J. S., and Hao, J.: Impact Assessment of Ammonia Emissions on Inorganic Aerosols in East China Using Response Surface Modeling Technique, *Environmental Science & Technology*, 45, 9293-9300, 10.1021/es2022347, 2011.
Wang, Y., Zhang, Q. Q., He, K., Zhang, Q., and Chai, L.: Sulfate-nitrate-ammonium aerosols over China: response to 2000–2015 emission changes of sulfur dioxide, nitrogen oxides, and ammonia, *Atmos. Chem. Phys.*, 13, 2635-2652, 10.5194/acp-13-2635-2013, 2013.
- 1145 Warner, J. X., Dickerson, R. R., Wei, Z., Strow, L. L., Wang, Y., and Liang, Q.: Increased atmospheric ammonia over the world's major agricultural areas detected from space, *Geophysical Research Letters*, 44, 2875-2884, <https://doi.org/10.1002/2016GL072305>, 2017.
Weber, R. J., Guo, H., Russell, A. G., and Nenes, A.: High aerosol acidity despite declining atmospheric sulfate concentrations over the past 15 years, *Nature Geoscience*, 9, 282-285, 10.1038/ngeo2665, 2016.
- 1150 Werner, M., Kryza, M., and Wind, P.: High resolution application of the EMEP MSC-W model over Eastern Europe – Analysis of the EMEP4PL results, *Atmospheric Research*, 212, 6-22, <https://doi.org/10.1016/j.atmosres.2018.04.025>, 2018.
WHO: World Health Organization global air quality guidelines: particulate matter (PM_{2.5} and PM₁₀), ozone, nitrogen dioxide, sulfur dioxide and carbon monoxide, World Health Organization, Geneva, 74-78, 2021.
- 1155 Xu, L., and Penner, J. E.: Global simulations of nitrate and ammonium aerosols and their radiative effects, *Atmos. Chem. Phys.*, 12, 9479-9504, 10.5194/acp-12-9479-2012, 2012.
- Yi, W., Shen, J., Liu, G., Wang, J., Yu, L., Li, Y., Reis, S., and Wu, J.: High NH₃ deposition in the environs of a commercial fattening pig farm in central south China, *Environmental Research Letters*, 16, 125007, 10.1088/1748-9326/ac3603, 2021.
- 1160 Yu, F., Nair, A. A., and Luo, G.: Long-Term Trend of Gaseous Ammonia Over the United States: Modeling and Comparison With Observations, *Journal of Geophysical Research: Atmospheres*, 123, 8315-8325, <https://doi.org/10.1029/2018JD028412>, 2018.
- Zheng, B., Tong, D., Li, M., Liu, F., Hong, C., Geng, G., Li, H., Li, X., Peng, L., Qi, J., Yan, L., Zhang, Y., Zhao, H., Zheng, Y., He, K., and Zhang, Q.: Trends in China's anthropogenic emissions since 2010 as the consequence of clean air actions, *Atmos. Chem. Phys.*, 18, 14095-14111, 10.5194/acp-18-14095-2018, 2018.
- 1165